

Hydrothermal fluids in epithermal and porphyry Au deposits in the Central Slovakia Volcanic Field

Book Chapter**Author(s):**

Koděra, Peter; Lexa, Jaroslav; Fallick, Anthony E.; Wälle, Markus; Biroň, Adrián

Publication date:

2014

Permanent link:

<https://doi.org/10.3929/ethz-b-000095427>

Rights / license:

[In Copyright - Non-Commercial Use Permitted](#)

Originally published in:

Geological Society, London, Special Publications 402(1), <https://doi.org/10.1144/SP402.5>

This is the Open Access version of: Koděra, P., Jaroslav, L., Fallick, A.E., Wälle, M, Biroň, A., 2014. Hydrothermal fluids in epithermal and porphyry Au deposits in the Central Slovakia Volcanic Field. *Geological Society, London, Special Publications*, vol. 402, pp. 177–206. <https://doi.org/10.1144/SP402.5>

Hydrothermal fluids in epithermal and porphyry Au deposits in the Central Slovakia Volcanic Field

Peter Koděra^{1*}, Jaroslav Lexa², Anthony E. Fallick³, Markus Wälle⁴, Adrián Biroň⁵

¹Department of Geology of Mineral Deposits, Faculty of Natural Sciences, Comenius University, Mlynská dolina, 842 15 Bratislava, Slovakia

²Geological Institute, Slovak Academy of Sciences, Dúbravská cesta 9, 840 05 Bratislava, Slovakia

³Scottish Universities Environmental Research Centre, East Kilbride, G75 0QF Glasgow, UK

⁴Department of Earth Sciences, ETH Zürich, 8092 Zürich, Switzerland

⁵Geological Institute, Slovak Academy of Sciences, Severná 5, 974 01 Banská Bystrica, Slovakia

*Corresponding author (e-mail: kodera@fns.uniba.sk)

Abstract

The Neogene Central Slovakia Volcanic Field in the Carpathian arc contains various Au deposits, hosted by central zones of large andesite stratovolcanoes. Fluids involved in mineralization have been studied at three different types of deposit, mostly by fluid inclusion and stable isotope techniques. Rozália mine in the Štiavnica stratovolcano hosts intermediate sulphidation style Au-Ag epithermal mineralization in subhorizontal veins, related to hydrothermal activity during an early stage of caldera collapse. Associated fluids of low salinity underwent extensive boiling at 280–330°C on transition from suprahydrostatic towards hydrodynamic conditions at shallow depths (~550 m) from fluids of mixed magmatic and meteoric origin. Kremnica ore field hosts a large system of low sulphidation style Au-Ag veins contemporaneous with rhyolite magmatism and situated on resurgent horst faults. Fluids were of low salinity, predominantly of meteoric origin and showed gradual decrease in temperature along the system (~270–140°C) related to decrease in erosion level from ~500 to ~50 m. Biely Vrch Au-porphyry deposit in the Javorie stratovolcano is associated with quartz stockwork in diorite porphyry intrusion. The major type of ore-bearing fluid was high temperature magmatic vapour (720 to <380°C) accompanied by Fe-rich salt melt. Gold precipitated in a high-temperature but low-pressure subvolcanic environment.

1. Introduction

Precious metal mining in central Europe has a long history, dating back over more than two thousand years. Major mining centres in the Neogene Central Slovakia Volcanic Field were one of the leading world producers of gold and silver in the 14th and 15th century (Bakos *et al.* 2004). Today gold mining remains in progress and new economic deposits are still being discovered. The most important gold-bearing deposits are hosted by central zones of large stratovolcanoes, hosting various types of hydrothermal mineralization, including porphyry and epithermal styles. During recent decades significant progress has been made in understanding of the mineralised paleohydrothermal systems in this region (e.g. Lexa *et al.* 1999a; Koděra *et al.* 2005, 2010a, 2010b; Koděra & Lexa 2010). The best studied localities include Rozália mine intermediate sulphidation epithermal Au-Ag deposit in the Štiavnica stratovolcano, Kremnica low sulphidation epithermal Au-Ag deposit in the Kremnické Vrchy Mts., and the recently discovered Biely Vrch Au-porphyry deposit in the central zone of the Javorie stratovolcano. This article represents a summary of the current knowledge of genesis of these gold-bearing hydrothermal systems, particularly focusing

on properties of associated ore-bearing fluids. It consists of a review of previously published data (Rozália mine) supplemented by new data (Kremnica, Biely Vrch) with the aim to show the variability of hydrothermal fluids associated with three different types of economic Au mineralisations within one volcanic field.

2. Regional geological setting

The Central Slovakia Volcanic Field is situated on the inner side of the Carpathian arc that is a part of the northern branch of the Alpine orogenic belt of Europe and covers over 5000 km² in area (Fig 1; Konečný *et al.* 1995). During the Neogene, the Carpathians represented an advancing continental margin to island arc that migrated north-eastward at the expense of subducting oceanic crust of flysch basins, until it collided gradually with the passive margin of the European platform (Royden *et al.* 1982). Advance of the arc caused by subduction roll-back was compensated by back-arc extension involving upwelling of asthenosphere. Volcanic rocks of Middle Miocene age (16.5 - 8.5 Ma) are closely associated with basin and range extension tectonics (Lexa & Konečný 1998; Konečný *et al.* 2002). Calc-alkaline rocks show the medium- to high-K trend similar to andesites of continental margins or evolved island arcs involving older continental crust (Lexa *et al.* 1998a). Isotopic data point to a mantle source for the magmas with considerable crustal contamination (Salters *et al.* 1988). Harangi & Lenkey (2007) as well as Seghedi & Downes (2011) concluded that the primary magmas were formed during the peak phase of extension by melting of previously metasomatized, enriched lithospheric mantle. Further evolution of magmas towards andesitic composition took place by high-pressure fractionation at the base of the crust, and by low-pressure fractionation, assimilation and mixing in shallow magma chambers towards dacitic composition. Associated crustal anatexis led to the evolution of anatectic rhyolitic magmas (Lexa *et al.* 1998a).

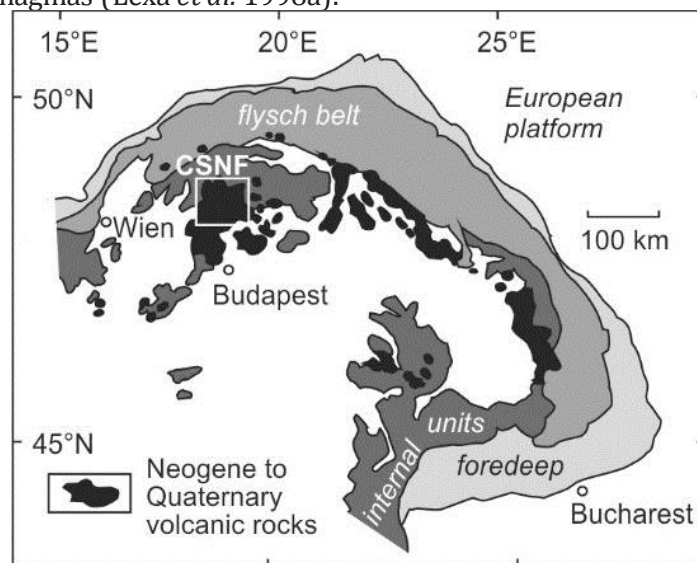


Figure 1. Position of the Central Slovakia Volcanic Field (CSVF) among the Neogene to Quaternary volcanic rocks in the area of Carpathian arc and Pannonian basin (after Lexa *et al.* 1999a).

Volcanic rocks in the Central Slovakia Volcanic Field evolved variably in a shallow marine or terrestrial environment (Konečný *et al.* 1995). Extrusive domes with extensive brecciation, breccia flows, lava flows with hyaloclastite breccias, and epiclastic volcanic conglomerates and sandstones dominate among submarine volcanic rocks. Stratovolcanoes of variable complexity from simple monogenous cones to compound volcanoes with volcanotectonic depressions and subvolcanic intrusive complexes are characteristic of the terrestrial environment. Central zones of former stratovolcanoes are indicated by subvolcanic intrusive complexes with intense alteration and by extrusive domes of differentiated rocks (Fig. 2 a). The tectono-thermal activation of the back-arc basins related to the thinning of the crust and lithosphere, and updoming of the

asthenosphere to shallow level, played an important role in magma generation as well as in metallogenetic processes. The coincidence of increased heat flow, magmatic activity, and back-arc extension creating pathways for hydrothermal fluids, were crucial factors. Gold-bearing mineral deposits in the Central Slovakia Volcanic Field are hosted by the central zones of large andesite stratovolcanoes involving volcanotectonic depressions, resurgent horsts, extensive subvolcanic intrusive complexes, and complexes of differentiated rocks (Fig. 2 *b*). Štiavnica stratovolcano, Javorie stratovolcano and Kremnické Vrch Mts are recognised as major centres of hydrothermal activity. They include Au- and Cu-Au porphyry and porphyry/skarn magmatic-hydrothermal systems related to small porphyry stocks of granodiorite to diorite composition, and intermediate to low sulphidation Au-Ag±Pb-Zn-Cu epithermal veins and Carlin-like sediment-hosted Au-occurrences related to horst-graben extension tectonics and associated fluid flow.

3. Analytical methods

New analytical data for Kremnica and Biely Vrch deposits include fluid inclusion microthermometry, stable isotope analyses and XRD analyses of altered rocks.

Fluid inclusions were studied using doubly polished wafers (~200 µm thick). The observed inclusions were assigned a probable primary or secondary origin according to the criteria of Roedder (1984). Due to the lack of clear fluid inclusion assemblages in the studied material (in the sense of Goldstein and Reynolds 1994) mostly individual inclusions have been measured. The thermometric behaviour of fluid inclusions was studied on a Linkam THMSG-600 heating-freezing stage at the State Geological Institute of Dionýz Štúr, Slovakia. The equipment was calibrated with natural fluid inclusions with pure CO₂ (-56.6°C), pure water (0°C) and inorganic standards (K₂Cr₂O₇, 371°C). The precision and accuracy of the microthermometric measurements, based on standard calibration procedures, is estimated as ± 0.2°C for the freezing runs and ± 3°C for the heating runs. Salinity estimates are based on the last melting temperatures of ice in the system NaCl-H₂O (Bodnar 1993) or in the system CaCl₂-H₂O (Steele-MacInnis et al. 2010) and on the halite melting temperatures in the system NaCl-H₂O ($T_{m,hal}$; Sterner et al. 1988).

Oxygen and hydrogen isotope compositions of minerals and fluid inclusions were analysed at the Scottish Universities Environmental Research Centre. Minerals were isolated using standard separation techniques, with the purity checked by XRD analyses where necessary. Water was extracted from 40 to 80 mg of hydrous minerals and converted to H₂ over chromium at 800°C. The yield was measured manometrically prior to D/H assay. For ¹⁸O/¹⁶O measurement, 1 mg of oxygen bearing samples reacted with chlorine trifluoride using laser heating. The oxygen isotope laser fluorination technique has been described by Macaulay et al. (2000), and the hydrogen isotope method by Fallick et al. (1993). The ¹⁸O/¹⁶O and ¹³C/¹²C ratios in carbonates were determined from CO₂ released by reaction with phosphoric acid. Calcite samples were reacted at 25°C and an oxygen isotope fractionation factor between calcite and CO₂ of 1.01025 was used. The precision of determinations by laboratory replicate analysis is 0.2 ‰ for δ¹⁸O, 0.2 ‰ for δ¹³C and 3 ‰ for δD at one sigma.

The samples used for clay mineralogy were crushed, subsequently ground and sieved under 0.16 mm and then treated chemically following the standard procedure of Jackson (1975) with separation of < 2 µm fractions by gravity settling. XRD analyses of clay fractions were performed on a Philips PW1710 diffractometer using CuKα radiation (40 kV, 20 mA) and a diffracted beam graphite monochromator. The identification of the mixed-layer illite-smectite and measurements of the percentage of expandable component layers (%S) were performed by peak-position methods (Środoń 1980, 1984; Dudek & Środoń 1996) on XRD patterns obtained from oriented, glycolated preparations of <2 µm fractions.

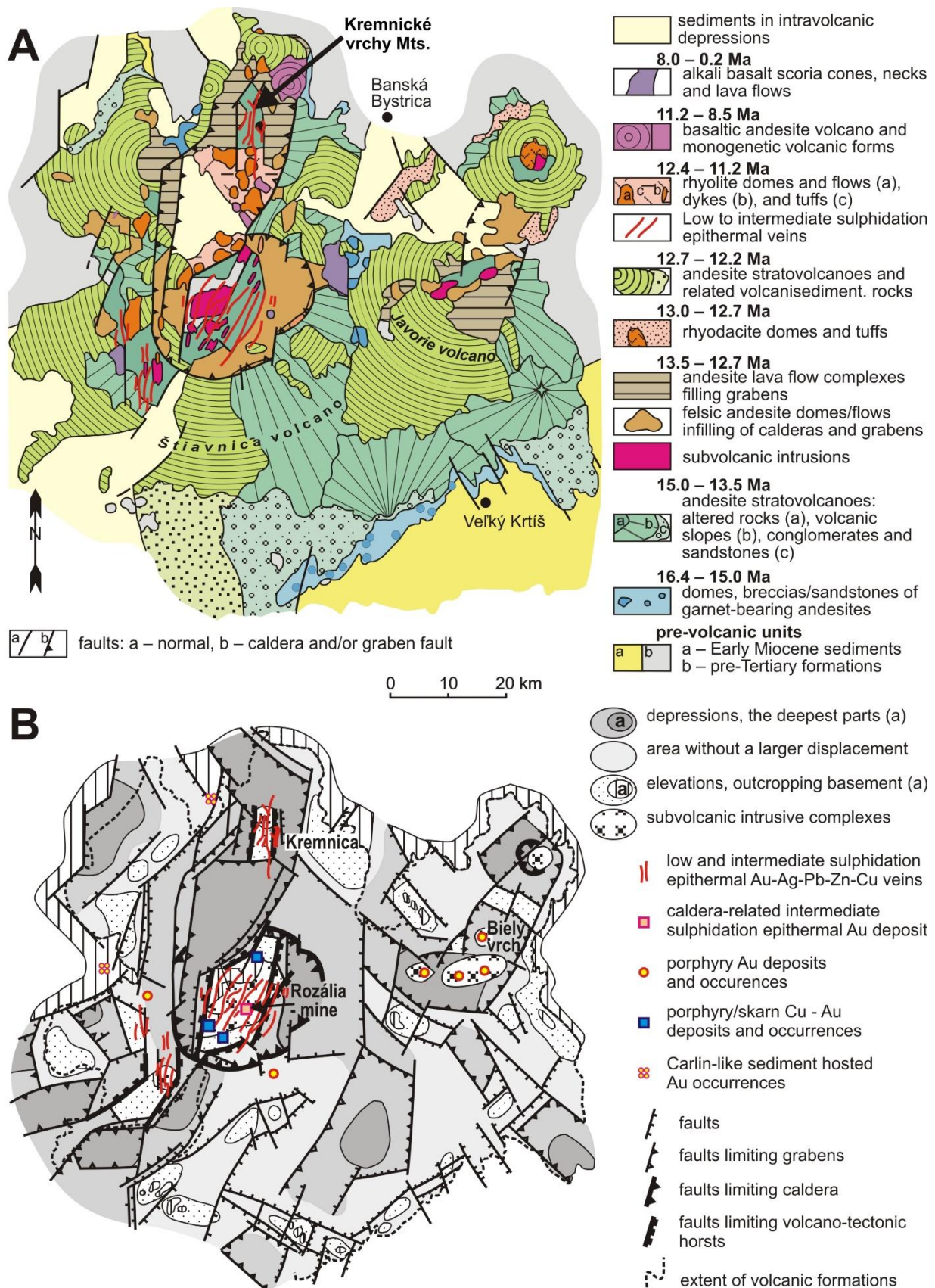
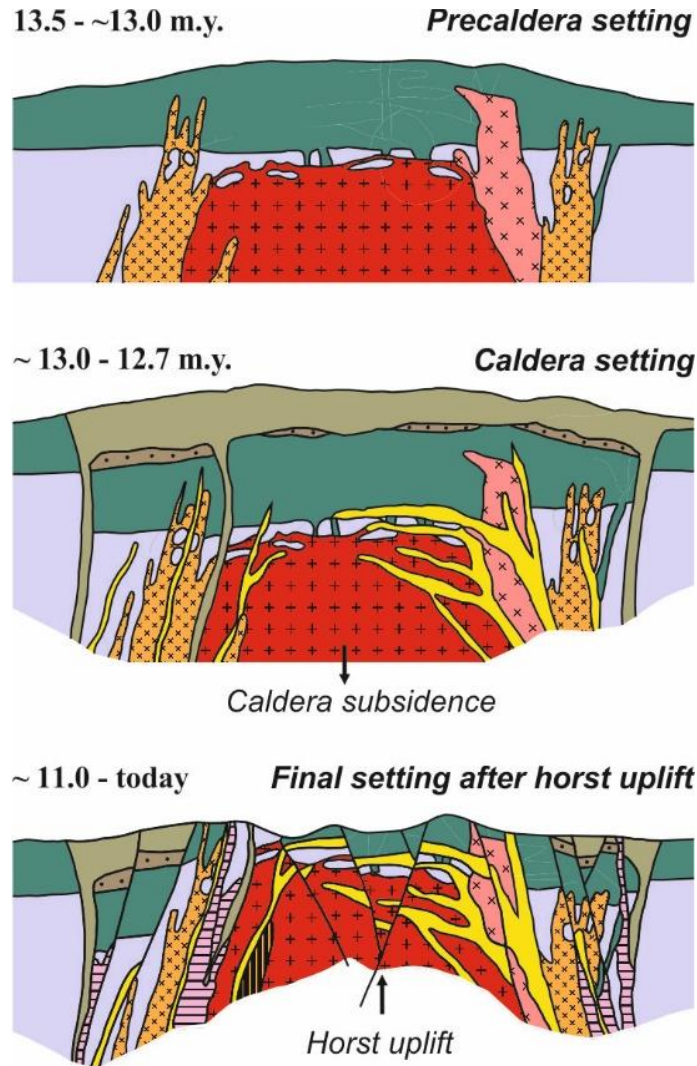
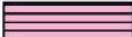



Figure 2. Regional geological setting and metallogeny of the study area: **(A)** Structure of the Central Slovakia Volcanic Field (after Konečný *et al.* 1995); major volcanic structures hosting ore districts (Štiavnica stratovolcano, Javorie stratovolcano and Kremnické Vrchy Mts) are indicated. **(B)** Basement structure and metallogenetic scheme of major Au-bearing deposits and occurrences in the Central Slovakia Volcanic Field (after Lexa 2000). Labelled marks on the map represent localities described in the text.




Post-caldera stage - 12.2 – 11.4 Ma


 Rhyolite dykes, extrusive domes


Caldera filling - 13.1 – 12.7 Ma

 Felsic andesite domes/flows and volcanoclastic rocks

 Caldera lake deposits

Subvolcanic intrusive complex - 13.5 – 12.9 Ma


 Quartz-diorite porphyry sills (a) and dykes (b)

 Dyke clusters/stocks of granodiorite/quartz-diorite porphyry

 Granodiorite pluton

 Diorite intrusion

Pre-caldera stage - 15.0 – 13.5 Ma

 Px and Px-Am andesites and andesite porphyry

 **Prevolcanic basement rocks**

Figure 3. Major stages in evolution of the Štiavnica stratovolcano central zone (after Lexa et al. 1999a and Koděra et al. 2005). Ages are based on Chernyshev et al. (2013).

4. Au-mineralization in Štiavnica stratovolcano

The Štiavnica stratovolcano is situated in the southern part of the Central Slovakia Volcanic Field. This stratovolcano with a diameter of almost 50 km covers some 2000 km² and is the largest volcano in the whole Carpatho-Pannonian area. An extensive caldera 20 km in diameter, a voluminous subvolcanic intrusive complex and a late-stage resurgent horst in the caldera centre accompanied by rhyolite volcanites are the most characteristic features (Fig. 2 *a*; Konečný *et al.* 1995). As the horst uplift was asymmetric, erosion in its NW part has reached basement rocks and subvolcanic intrusions of diorite, granodiorite and granodiorite to quartz-diorite porphyry. The stratovolcano hosts one of the largest ore districts in the Carpathian arc, famous for its long-lived silver and gold mining at least from the early Middle Ages.

According to Konečný *et al.* (1998b) evolution of the Štiavnica stratovolcano occurred in five stages during the interval 15.0 to 11.2 Ma (Chernyshev *et al.* 2013; Fig. 3). Its evolution started with formation of a large andesite stratovolcano (15.0 – 13.5 Ma), involving late stage andesite to diorite porphyry intrusions accompanied by uneconomic Au-porphyry mineralization at several localities (Bakos *et al.* 2010). During subsequent denudation of the stratovolcano, emplacement of several subvolcanic intrusions took place during the pre-caldera stage (13.5 – 12.9 Ma), including a diorite pluton with associated barren advanced argillic lithocap (Lexa *et al.* 1999a), an extensive granodiorite pluton responsible for development of intrusion-related Fe-skarn and base metal stockwork systems (Koděra *et al.* 2004) and granodiorite porphyry stocks hosting Cu-Au porphyry/skarn systems (Koděra *et al.* 2010b). Subsequent caldera subsidence and emplacement of quartz-diorite porphyry sills and dykes (13.1 – 12.7 Ma) is known to coincide with epithermal Au-mineralization in subhorizontal veins (Rozália mine; Koděra *et al.* 2005) and hot-spring type mineralization occurrences (Lexa *et al.*, 1999a). Renewed andesitic volcanism took place during the post-caldera stage (12.7 – 12.2 Ma). Final long-lasting resurgent horst uplift in the centre of the caldera was associated with rhyolitic volcanic activity (12.2 – 11.4 Ma) and evolution of an extensive system of intermediate to low sulphidation veins (12.2 – 10.7 Ma) with considerable historical production of Ag-Au±Pb-Zn-Cu (Onačila *et al.* 1995; Lexa *et al.* 1999a).

4.1. Epithermal Au-Ag mineralization of subhorizontal veins in the Rozália mine

This type of mineralization is currently the only working Au mine in this mining district but also in the whole of central Europe. Since 1992 it has produced roughly 5 t of gold (Slovak Minerals Yearbooks 2003, 2008, 2011) and an equal amount of gold is in estimated remaining resources. Average ore grade varies between 7 and 10 g/t Au. It was unexpectedly discovered in 1988 during exploration for continuation of steep, horst-uplift related epithermal base metal veins at deep levels of the historic Rozália base metal mine in Banská Hodruša (400-650 m below surface). This was recognised as the relatively oldest epithermal vein system in the district and has developed within subhorizontal structures associated with a caldera collapse-related stress field (Koděra *et al.* 2005). The Au mineralization typically occurs in banded veins and veinlets and in silicified hydrothermal breccias at the base of pre-caldera andesites, close to the roof of a subvolcanic granodiorite intrusion (Fig. 4). The veins are dismembered by a set of quartz-diorite porphyry sills and displaced by the younger, steeply-dipping, Rozália base-metal vein, and parallel structures related to resurgent horst uplift in the caldera centre. Porphyry sills are mostly parallel to low-angle mineralised structures. The mineralised andesites have been pervasively silicified, while illite, pyrite, minor adularia and carbonates are also present.

Three stages of mineralization are recognised at the deposit (Maťo *et al.* 1996; Šály *et al.* 2008; Kubač, 2013). Stage 1 corresponds to pervasive silicification and pyritization, and involves the formation of early subhorizontal veins with milky quartz and silicified breccias of low Au grade (0.3-5.5 ppm). Quartz is accompanied by carbonates (Mn-calcite, Fe-dolomite, siderite), minor sphalerite and rare gold of high fineness (90.5-95.8 % Au). Stage 2 is represented by quartz, rhodonite, carbonates (rhodochrosite/Mn-calcite, Fe-dolomite, siderite), pyrite, gold of lesser fineness (80.6-87.8 % Au), FeS-poor sphalerite, galena, chalcopyrite, petzite and hessite. Gold is

associated with base-metal-enriched parts of veins with up to 600 ppm Au (Koděra *et al.* 2005). Stage 3 represents an overprint by mineralization associated with horst uplift and includes quartz, Fe/Ca carbonate, pyrite, low FeS sphalerite, galena, chalcopyrite, tetrahedrite, polybasite, hessite, and gold of low fineness (73.9-78.8 % Au - electrum). The thickness of individual veins is between 0.1-2 m with gold contents varying from 5 to 600 g/t, and averaging 20 to 50 g/t, with Ag/Au ratio varying from 1:2 to 10:1, depending on the mineralization stage. Native gold of microscopic size is the dominant form of gold (Maťo *et al.* 1996). Most of the gold at the deposit was introduced during Stage 2, whereas during Stage 3 some gold was remobilised as indicated by slight enrichment in gold of the Rozália vein in places where it crosscuts the earlier Au-mineralisation (Koděra *et al.* 2005).

Principal characteristics of the deposit are indicative of epithermal mineralisation of intermediate sulphidation-style (Sillitoe & Hedenquist 2003): sericite and minor adularia are the key alteration minerals, mineralisation contains common base metal sulphides and Mn-varieties of carbonates and main metals include Au, Ag, Zn, Pb, Cu.

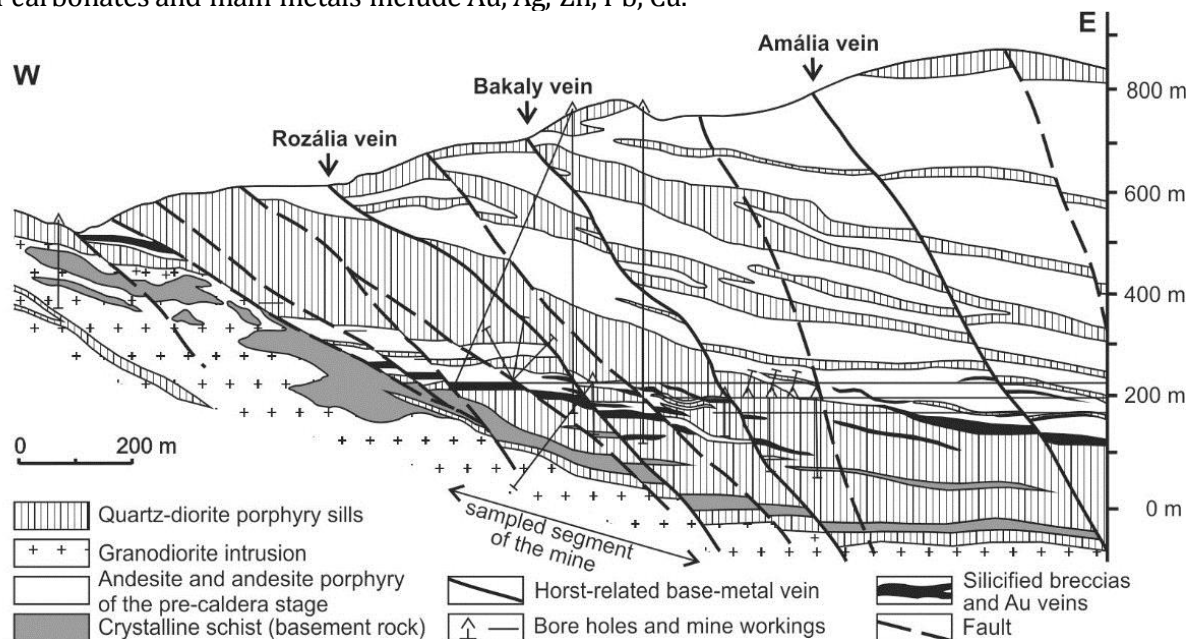


Figure 4. Simplified cross section of the intermediate sulphidation epithermal Au deposit at the Rozália mine in the central zone of the Štiavnica stratovolcano (after Šály & Prcúch 1999, and Šály *et al.* 2008)

4.2. Fluid inclusion data

Fluid inclusion microthermometry data were collected from fluid inclusions in quartz, sphalerite and carbonate minerals from vein filling (Koděra & Lexa 2003; Koděra *et al.* 2005). Three types of aqueous inclusions could be distinguished: two-phase liquid-rich, two-phase vapour-rich and three-phase liquid-rich with a halite crystal (Fig. 5 *d*). Boiling of fluids is indicated by common coexistence of vapour-rich and liquid-rich inclusions. High salinity liquid-rich inclusions and halite-bearing inclusions occur only in samples showing strong evidence of boiling and are secondary with respect to host quartz (Figs. 5 *c, d*). Liquid-rich inclusions locally contain fibrous sericite interpreted as a captured phase.

Fluid inclusions hosted in *Stage 1* minerals show a relatively broad range of homogenization temperatures (T_h) and salinities, but most data fall within 280 to 330°C and 0-3 wt% NaCl eq. (Fig. 6 *a*). Clear evidence of boiling was documented in at least one sample, where high T_h values result from heterogeneous trapping of vapour and liquid. The presence of NaCl and some other salts (KCl, MgCl₂, FeCl₂) is indicated by measured eutectic temperatures in two/phase liquid-rich inclusions (T_e ; -37 to -21°C); however, halite-bearing aqueous inclusions show the presence of CaCl₂ (T_e down to -52°C; Shepherd *et al.* 1985). The high-salinity inclusions, that accompany the populations of inclusions with evidence for boiling within the Au deposit samples, can result from boiling near to dryness (Shepherd *et al.* 1985). This interpretation is further supported by the

associated trend of decreasing total homogenization temperatures with increasing salinity (Figs. 6 *a, b*), as the decrease in T_h values can be explained by adiabatic cooling that accompanies boiling. This phenomenon occurs in open boiling systems, where liquid is immobilized in pores and microfractures whereas the vapour escapes (Simmons & Browne 1997). The observed increase in salinity due to boiling requires removal of 90 to 99 % of the liquid as vapour. Alternatively, high salinity fluid inclusions can be explained by episodic injections of formation waters or magmatic brines (Simmons 1995), but such interpretations are unlikely due to the absence of thick sequences of sedimentary rock and the absence of significantly increased T_h values of the brines, respectively.

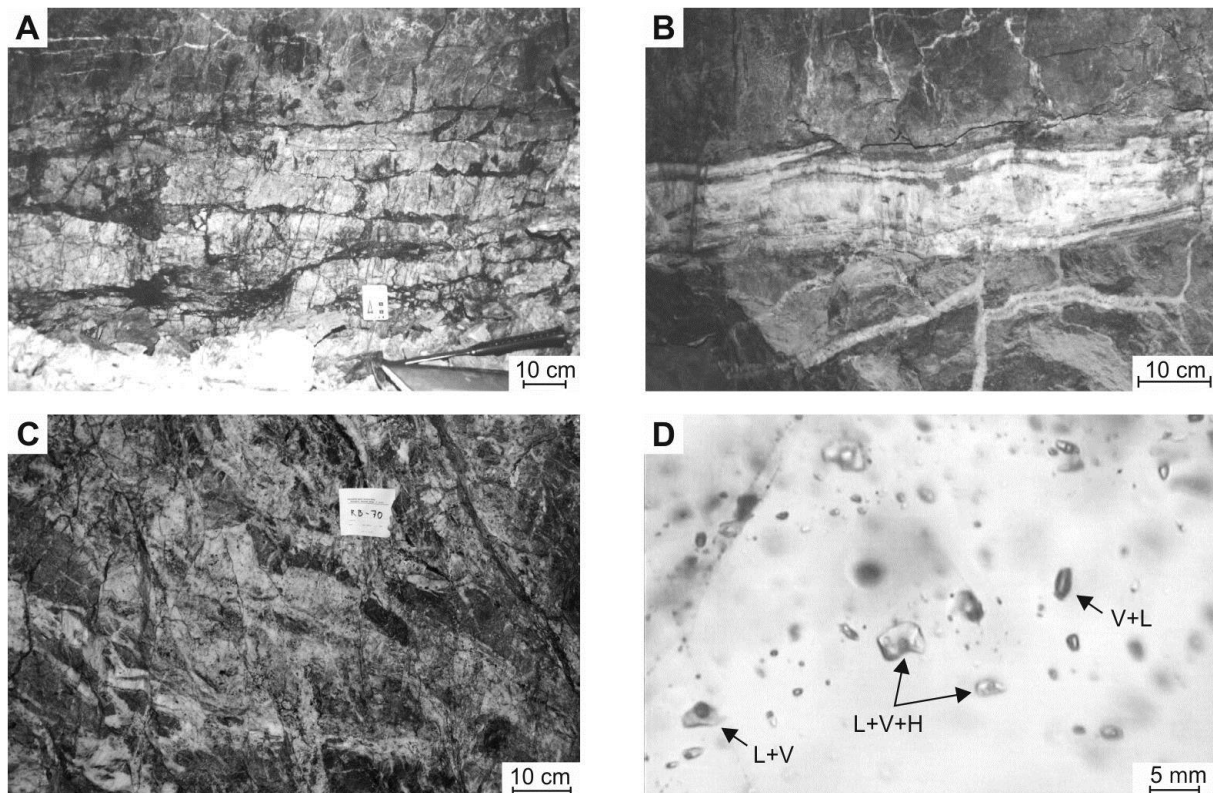


Figure 5. Major textural features and typical fluid inclusions of the Rozália mine epithermal Au deposit (after Koděra *et al.* 2005). (A) Fractured subhorizontal barren quartz vein of the 1st stage of Au mineralization. (B) Typical subhorizontal banded Au-rich vein of the 2nd stage in andesite. (C) 2nd stage quartz-carbonate vein showing multiple hydraulic fracturing. (D) Typical fluid inclusions hosted in vein quartz: L+V - two-phase, liquid-rich inclusion; V+L - two-phase, vapour-rich inclusion; L+V+H -three-phase, liquid-rich inclusion with halite crystal.

Microthermometric analyses of the *Stage 2* samples also show a broad range of salinities and T_h values, whereas most of the measured values belong to ranges 0 to 4 wt% NaCl eq. and 250 to 310°C, respectively (Fig. 6 *b*). Evidence of boiling of fluids was recognized in most of the samples studied, supported by increased T_h values and salinities. Traces of pure CO₂ were occasionally detected in some vapour-rich inclusions (CO₂ melting temperature -56.6°C). More variable composition of aqueous liquids is indicated by large range of T_e values (-55 to -22°C), but increased contents of CaCl₂ and/or FeCl₂ (low T_e values) are again affiliated to greater salinity inclusions. Homogenisation temperatures of most fluid inclusions in sphalerite show slightly cooler T_h values (250-280°C) compared with those in quartz (280-300°C) and carbonates (290-310°C).

Except for the few brine fluid inclusions resulting from extreme boiling, the diagrams of combined T_h and salinity data (Fig. 6 *a, b*) show apparent trends of changing salinity at relatively constant T_h values. Such trends are indicative of isothermal mixing of fluids with contrasting salinity, such as magmatic and heated meteoric waters, which is typical for low and intermediate sulphidation epithermal systems (Hedenquist & Lowenstern 1994; Simmons *et al.*, 2005). Rare low T_h values (as low as 183°C) probably represent an overprint of some late-stage, much cooler fluids,

possibly associated with the final mineralization stages of the younger horst uplift-related Rozália vein.

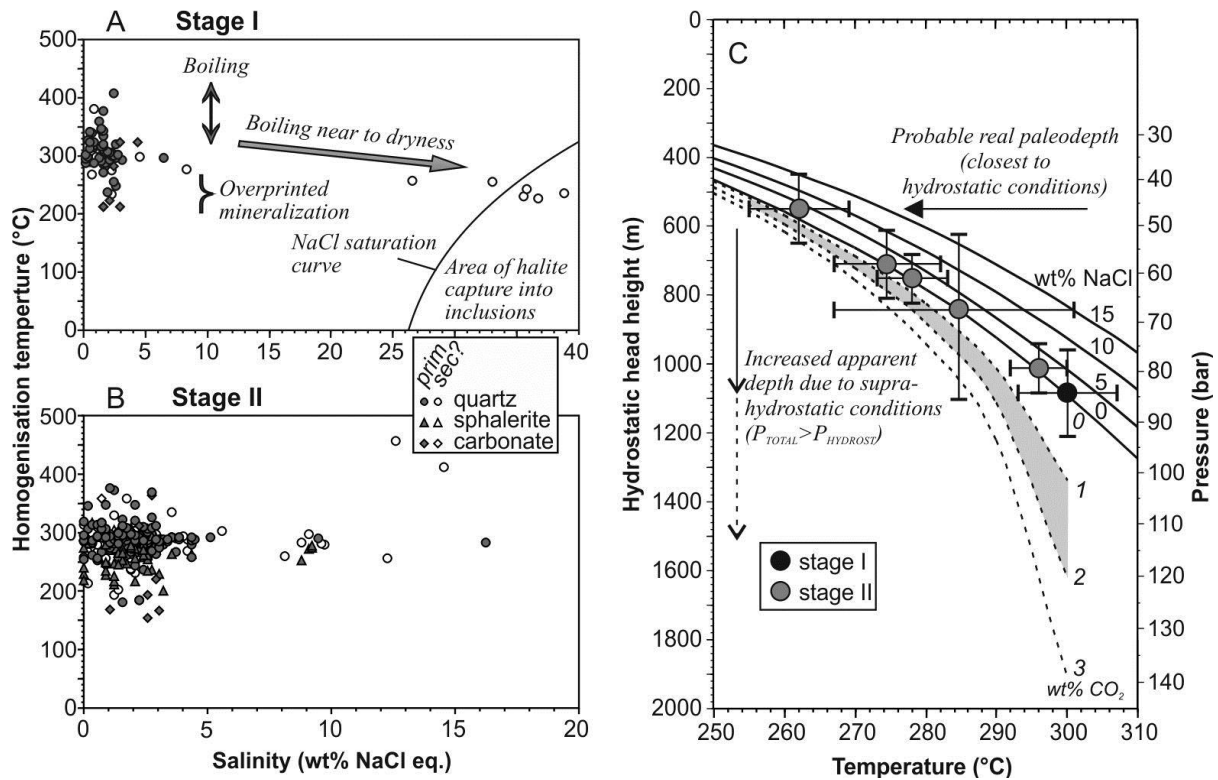


Figure 6. Microthermometry data from fluid inclusions of the Rozália mine epithermal Au deposit and their interpretation (after Koděra et al. 2005). (A-B) Plots of liquid-vapour homogenization temperatures vs. salinity for fluid inclusions in minerals from both major stages of Au mineralization. Presence of high salinity inclusions with progressively decreasing Th is indicative of boiling near to dryness. Note the different salinity scales. (prim = primary, sec? = possibly secondary origin). (C) Boiling point curves showing estimated boiling conditions of fluids related to the studied deposit. Curves for the H₂O-NaCl system are constructed using the data of Haas (1971, 1976). Curves for the H₂O-CO₂-NaCl system are constructed according to the methods and equations of Wilkinson (2001) based on an initial temperature of 300°C, 0 to 3 wt% CO₂ and 0.5m NaCl (~2.8 wt%). Estimates of minimum pressures and corresponding hydrostatic head heights for samples with inclusion populations with evidence of boiling are based on the H₂O-NaCl system. Error bars represent variation of minimum homogenization temperatures, salinities and corresponding pressures for individual samples showing evidence of boiling. Shaded area corresponds to typical concentrations of CO₂ in low-sulphidation precious-metal mineralizations.

The fluid inclusion data for populations with evidence for boiling were used to calculate fluid pressures and depth of formation of the studied mineralization in the system H₂O-NaCl (Fig. 6 c; Haas 1971, 1976). Stage 1 inclusion data resulted in pressures from 77 to 95 bars probably corresponding to initial opening of host fractures, when the hydrothermal system was governed by suprahydrostatic conditions, i.e. it was not connected to the surface. Brecciation and silicification, commonly observed in the main Svetozár vein and parallel vein structures are the result of local overpressure. Stage 2 data produce substantially lower, but highly variable, pressures (39 to 87 bars) indicative of opening of the system and a transition to dominantly hydrodynamic conditions, with pressure release resulting in extensive boiling. Continuous boiling is known to induce a substantial decrease in solubility of gold, which precipitates accompanied by adularia and rhodochrosite (Seward 1989; Hedenquist & Arribas 1999; Simmons et al., 2005). Decrease in permeability and redevelopment of greater fluid pressure is likely to occur due to sealing of fractures by continued mineral deposition (Fournier 1999). Thus, the variable pressures probably correspond to repeated cycles of pressure and stress build-up, fracturing, and mineral deposition ("crack-seal mechanism"; e.g. Sibson *et al.* 1988; Boullier & Robert 1992). The calculated minimum depths (hydrostatic column heights) range from 960 to 1210 m for stage 1, and 450 to 1105 m for stage 2 samples. The large variability in calculated apparent depths cannot result from variability in position of individual samples because of the very shallow angle of the

hosting structures. The exact position (paleodepth) of individual samples could not be reconstructed due to complex displacement by younger faults and porphyry sills; however, Figure 4 shows that the maximum possible differences in depth could not exceed 50 m along the veins in the sampled area. In addition, the presence of CO₂ (possibly up to 2 wt%; Hedenquist & Henley 1985; Hedenquist *et al.* 1996) can, if neglected, cause significant underestimates of depth, especially during the early stage of boiling, although continuous boiling would release most of the dissolved CO₂ and reduce this effect. However, suprahydrostatic conditions have the opposite effect of overestimating the apparent depth, if neglected. In conclusion, the differences in apparent depth probably correspond to changes in fluid pressure. During stage 1 the fluid pressure was relatively high, governed by suprahydrostatic conditions and by the probable effect of CO₂, but during Stage 2 the pressure was significantly decreased due to opening of the system and release of CO₂. The real paleodepth (550 m ± 100 m) can be derived from lowest fluid pressure (47 ± 7 bar) which was obtained from one of the Stage 2 samples and corresponds to the fluid that was closest to CO₂-poor hydrostatic conditions.

4.3. Stable isotope data

Quartz and carbonate from veins were analyzed for their O, H and C isotope compositions, as appropriate. The δ¹⁸O values of hydrothermal fluids coexisting with quartz and calcite and δ¹³C of CO₂ in equilibrium with calcite were calculated using fractionation factors of Matsuhisa *et al.* (1979), Friedman & O'Neil (1977) and Chacko *et al.* (1991), respectively, applying temperatures derived from fluid inclusion microthermometry (Koděra *et al.* 2005). The obtained O and H isotope data showed a relatively homogeneous fluid composition, similar for both stages of mineralization (Stage 1: -2.7 to +1.1 ‰ δ¹⁸O; Stage 2: -78 to -62 ‰ δD; Fig. 7). The plot of combined δ¹⁸O_{fluid} and δD_{fluid} values probably indicates a mixed character of fluids falling between the fields of typical magmatic water dissolved in felsic melts (Taylor 1992) and meteoric waters. However, fluid-rock oxygen isotope exchange also could have considerably influenced the composition of fluids, resulting in a δ¹⁸O_{fluid} shift of meteoric waters from the meteoric water line (Taylor 1997). In such a case, the O-shift is not accompanied by a mass-balance-controlled δD_{fluid} shift, except when fluid/rock ratios are very low. Most likely, both fluid-rock oxygen isotope exchange and fluid mixing have occurred; however, well homogenised isotopic fluid composition is consistent with mixing with meteoric water taking place outside the deposit during ascent of magmatic fluids from depth (a deep-convecting source of meteoric fluids).

Vapour separation due to boiling could have resulted in changes of isotope composition of the remaining aqueous fluid. Boiling away of 90 % of liquid can result in a maximum enrichment of around 4 ‰ δ¹⁸O_{fluid} and a maximum relative depletion of 13 ‰ in δD_{fluid} (Horita & Wesolowski 1994). Thus the variation in the samples reported here, which are up to 3.8 ‰ for δ¹⁸O_{fluid} and 16 ‰ for δD_{fluid} can be related to end-stages of open-system boiling observed in some fluid inclusion populations.

Interestingly, the isotopic composition of fluids related to Au-mineralization is very different to those related to alteration of granodiorite pluton (Koděra *et al.* 2004) which is present in the footwall of the veins (Fig. 7). The fluids in equilibrium with granodiorite-related alteration minerals form a mixing trend between magmatic water and isotopically much heavier meteoric water, probably influenced by interaction with host-rock. The differences in composition may be related to changes in isotope composition of meteoric water over the timescale between the emplacement of granodiorite and formation of veins. According to the palynological data of Planderová *et al.* (1993), during the lifetime of the Štiavnica stratovolcano (15.0 to 11.2 Ma), the climate changed from humid subtropical, influenced by the sea lying to the south of the volcano (Konečný *et al.* 1995), towards a significantly cooler and drier climate without a proximal sea. Alternatively, lower δD_{fluid} values of epithermal veins may be also related to the method of fluid extraction. Faure (2003) has shown that δD values of water extracted from fluid inclusions from active geothermal systems are up to 30 ‰ more negative than δD of the geothermal water as the thermal decrepitation procedure can extract both fluid inclusion and structurally bound water from quartz (Simon 2001).

The isotopic composition of carbon in two calcite samples from the second stage of Au mineralization (-4.0 and -4.2 ‰ V-PDB $\delta^{13}\text{C}_{\text{CO}_2}$) are typical of carbonates from epithermal deposits (Field & Fifarek 1985). Various sources of carbon can account for such values, including atmospheric CO_2 in meteoric waters and carbon of deep-seated origin (Field & Fifarek 1985; Ohmoto & Goldhaber 1997).

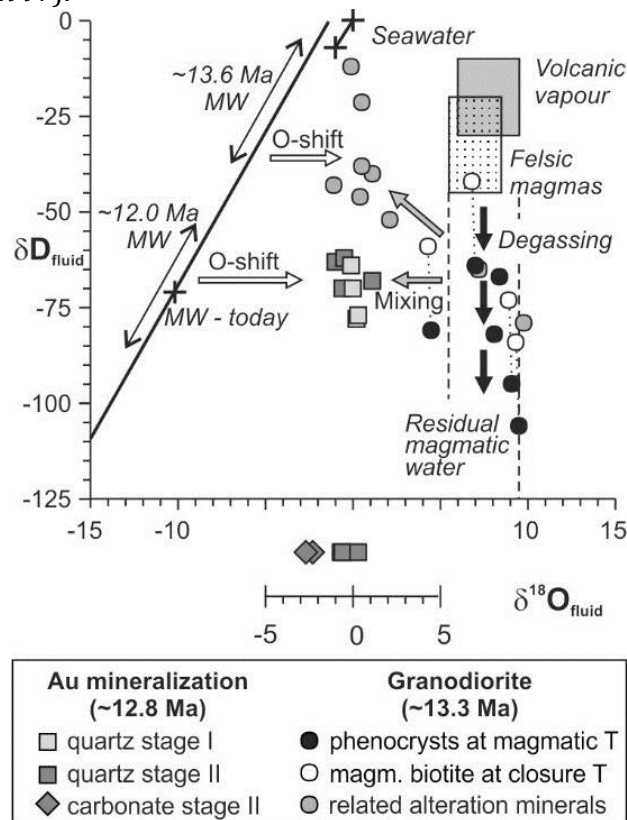


Figure 7. Isotopic composition of water in equilibrium with minerals and in fluid inclusions from the Rozália mine Au mineralization and hydrothermal alteration related to granodiorite intrusion (Koděra *et al.* 2004) in the vicinity of the Au deposit (after Koděra *et al.* 2005). Also shown are the most probable ages of Au-mineralisation and granodiorite (based on Chernyshev *et al.* 2013) and meteoric waters, corresponding to periods of changing climate during evolution of the Štiavnica stratovolcano (Planderová *et al.* 1993). The composition of water dissolved in felsic melts is based on Taylor (1992) and water discharged from high-temperature fumaroles from Giggenbach (1992). The seawater isotopic composition is given for recent SMOW (0, 0) and for deglaciated planet in Miocene (-1, -7) (Sheppard 1986). Today local meteoric water (MW) composition is based on data of IAEA (1992), composition of MW during the evolution of the Štiavnica stratovolcano is reconstructed based on paleoclimate information. Black arrows indicate δD depletion of residual magmatic water during open-system degassing that is preserved in magmatic phenocrysts (Taylor 1992; Hedenquist *et al.* 1998). Grey arrows indicate mixing trend of magmatic water with meteoric water of different composition, related to continuous change in climate. White arrows (O-shift) represent the possible effect of oxygen isotope re-equilibration by wall-rock interaction.

4.4. Genetic model

There have been several attempts to explain the position of the Rozália Au deposit in the evolution of the Štiavnica stratovolcano since its discovery, including affiliation to horst-related veins and granodiorite pluton (Maťo *et al.* 1996; Lexa *et al.* 1999b; Háber *et al.* 2001). However, only the most recent model is based on data from sample suites with well-constrained field and paragenetic location and careful interpretation of field observations, structural, fluid inclusion and stable isotope data (Koděra *et al.* 2005). The model proposes a genetic relationship to hydrothermal activity during the early stage of caldera collapse (Fig. 8). This relative timing is based on the age relationship with the surrounding rocks, and fluid properties of the mineralizing fluids.

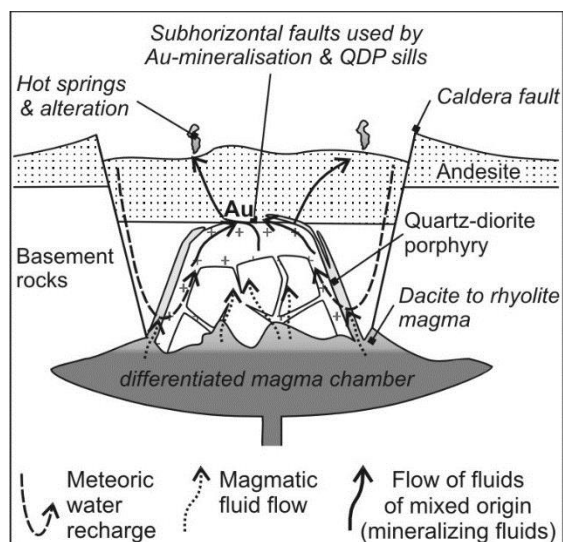


Figure 8. Genetic model of Au mineralization at Rozália mine in the central zone of the Štiavnica stratovolcano (after Koděra *et al.* 2005).

Geological evidence, supported by arguments based on stable isotope data, demonstrates that the Au mineralization is younger than the granodiorite and related hydrothermal systems, but older than most sills of quartz-diorite porphyries and resurgent horst-related epithermal veins. Furthermore, fluid inclusion data show a relatively shallow depth for Au mineralization ($550 \text{ m} \pm 100 \text{ m}$) compared to the estimated depth of emplacement of the granodiorite intrusion (2.5-4 km, Konečný 2002). There is no evidence for any other deep intrusions below the deposit that could be genetically related. The closest occurrence of mineralized porphyry stocks (Medené) is located more than 3 km from the Au deposit (Lexa *et al.* 1999a). The existence of hydrothermal activity during proposed timing of the deposit is clear from the presence of hot spring type alteration in caldera infill, for instance at the locality Červená Studňa, 2 km NE of the Au deposit (Lexa *et al.* 1999a).

The fluids responsible for the Au mineralization in the Rozália mine have characteristics typical of intermediate sulphidation epithermal Au deposits, including low to moderate salinities, moderate temperatures and extensive boiling (e.g. Hedenquist & Lowenstern 1994; Sillitoe & Hedenquist 2003). Data derived from fluid inclusion populations with evidence for boiling suggest significant changes in confining pressures related to continuous opening of the system and transition from suprahstatic to hydrodynamic conditions. Corresponding minimum depths calculated for hydrostatic pressure indicate a relatively shallow depth below the palaeosurface ($\sim 550 \text{ m}$), which coincides with the present vertical distance between the Au mineralization and the base of the caldera filling, which is roughly 500-600 m, if corrected for the thickness of post-mineralization porphyry sills and displacement on younger faults.

The hydrothermal fluids related to Au mineralization ascended along structures resulting from the same stress field that governed emplacement of the granodiorite pluton, quartz-diorite porphyry dykes and sills, and caldera collapse. This stress field, reflected by the sub-horizontal and low-angle extension structures, was influenced by the presence of a shallow magma chamber filled by magma of lower density than the overlying rocks (Lexa *et al.* 1999b). The caldera subsidence and related significant changes in hydrologic conditions established convective fluid flow paths using deep marginal caldera faults for infiltration, and using extensional structures in the central part of the caldera for major precipitation of minerals. The source of heat and magmatic components for the fluids was probably a differentiated, shallow, magma chamber below the base of the volcano. The chamber was also the source of magma for the post-mineralization sills and dikes of quartz diorite porphyries that used the same low-angle structures as the Au mineralization. Finally, during the latest stages of evolution of the volcano the resurgent horst formed in the centre of the caldera whereas the governing stress field produced a system of steep faults and epithermal veins, including the Rozália base-metal vein that cuts the Au deposit.

5. Au-mineralization in Kremnické Vrchy Mts.

The Kremnické Vrchy mountain range is situated in the northern part of the Central Slovakia Volcanic Field (Fig. 2). Volcanites include remnants of a large andesite stratovolcano with subvolcanic intrusive rocks in the central zone, a N-S trending graben with volcanic formations including differentiated rocks over 1000 m in thickness, remnants of 4 younger volcanoes situated next to marginal faults of the graben, a resurgent horst in the central part of the graben associated with late-stage rhyolite magmatic activity and sporadic occurrence of the youngest basalts and basaltic andesites (Lexa *et al.* 1998b).

The resurgent horst is built of the pre-graben propylitized andesite complex accompanied at depth by subvolcanic intrusions of gabbrodiorite, diorite, diorite porphyry and minor quartz-diorite porphyry (16.2-15.0 Ma; Lexa *et al.* 1998b). Emplacement of subvolcanic intrusions was accompanied by minor skarn/stockwork base metal mineralization (Böhmer 1977; Štohl *et al.* 1994). The horst is surrounded by andesitic rocks of graben fill (15.0-13.5 Ma). Eastern marginal faults of the horst host an extensive epithermal vein system, the Kremnica Au-Ag deposit. The structure of the horst is dominated by N-S and NE-SW trending normal faults, corresponding to the regional stress field with strong NW-SE extension during the interval 13.5-9 Ma (Nemčok *et al.* 1993). Uplift of the horst was contemporaneous with the epithermal mineralization (11.1-10.1 Ma on illite, 12.1-11.5 Ma on adularia; Kraus *et al.* 1999; Pécskay *et al.* 2010) and emplacement of rhyolite dykes with corresponding granite porphyry subvolcanic intrusions at depth. Fluid flow related to horst-graben extension tectonics resulted also in sediment-hosted Carlin-like Au and Hg mineralization occurrences (Remata and Malachov; Fig. 2 b) next to marginal faults of the graben.

Contemporaneous rhyolite domes, flows and volcanoclastic rocks, mostly tuffs (12.3-11.5 Ma; Pécskay *et al.* 2010) occur south of the horst in the northern part of the Žiar tectonic depression. This rhyolite complex is 200-400 m thick and represents the upper part of the depression infill (Lexa *et al.* 1998b). Underneath the complex tuffaceous sediments are present, except at its northern margin, where rhyolitic rocks rest directly on andesitic rocks of the graben fill.

5.1. Epithermal Au-Ag mineralization (Kremnica vein system)

The Kremnica gold deposit was one of the most important gold producers in Medieval Europe with at least one thousand years of mining history (Bakos *et al.* 2004; Finka 2009), considerable historical production of precious metals (~46 t Au and 208 t Ag; Finka 2009) and 25 Mt of ore reserves with 1.42 g/t Au (www.ortacresources.com). More than 120 veins are known within this deposit, grouped into two major vein systems (Figs. 9, 10).

The system of epithermal veins of low sulphidation type is represented by a major transtension/extension fault accompanied by low angle second order vein structures close to the surface, and complementary antithetic veins ("1st system"). In addition, in the hanging wall of the master lystric fault there is large complementary vein system ("2nd system"), underneath Kremnica town (Koděra *et al.* 2007).

The 1st vein system is dominated by the first order lystric fault, intruded also by rhyolite dikes, with the major vein segments called Kirchberg, Schindler-Teich and Šturec (Schrämen vein). The mineralised fault dipping 50°-60° gradually opens towards the surface to its maximum width of 80 m in the central part at Šturec (Fig. 10). The directional length of the 1st vein system attains roughly 6.5 km and vertical extent of veins exceeds 1200 m in the northern part of the system, but only their upper 200 – 300 m are enriched in precious metals (Böhmer *et al.*, 1977). However, the gold and silver contents decrease with increasing depth. Ore grades in the upper parts of veins usually vary over the range of 1-5 g/t Au and 5-30 g/t Ag (Böhmer 1966; Veľký 1992; Bartalský & Finka 1999). The main vein structure branches into a funnel-shaped system of veins and veinlets,

including complementary antithetic veins (Fig. 10). Vein filling is represented by banded and cavernous quartz, occasionally with carbonates. Mineralogical studies determined two major stages including 6 mineral associations (Böhmer 1966; Mat'ó 1997). The Au-Ag stage contains early minor barren carbonate substage (1), two quartz substages (2 and 3) and pyrite substage (4). Microscopic Au precipitated mostly during the pyrite substage and occurs as electrum or gold in pyrite and quartz in dark quartz-chalcedony bands with fine dispersed pyrite/marcasite. Pyrite and arsenopyrite are the most common ore minerals, accompanied by minor galena, sphalerite, chalcopyrite, proustite, pyrargyrite and Ag sulphosalts. In deeper parts of veins (250-1000 m in the northern part of the system) more common base metal sulphides are accompanied by rare tellurides. The Sb ± Hg, As stage was followed by intensive intermineralization tectonics and fills mainly fissures, especially in the hanging wall of the major vein structure. This stage includes quartz-carbonate substage (5) with predominant dolomite and minor quartz with rare disseminated sulphides, sulphosalts and electrum. Stibnite substage (6) with common stibnite, pyrite, marcasite in a quartz-chalcedony gangue is best developed in the footwall structures (mainly at Šturec). Extensive wall-rock alteration includes adularia, quartz, illite/smectite, kaolinite, passing outwards into chlorite, smectite, variably with disseminated pyrite and carbonate (Kraus et al. 1994).

The 2nd vein system represents a large scale complementary vein system with 40 veins in the hanging wall of the lystric master fault (1st system). In contrast to the 1st system the veins are much shorter (less than 1.5 km) and thinner (less than 2 m). Gold is typically present as visible aggregates (bonanza-type gold) in cavernous quartz-carbonate gangue with up to 1 % of Au, but average grades were just ~4 g/t Au and 30 g/t Ag. The richest Au concentrations were in ore shoots, stringers and vein intersections. Evolution of mineral paragenesis was similar to the 1st vein system except for the absence of the 1st (carbonate) substage and a lesser extent of the 2nd stage of mineralization. Gold was introduced mostly during the 2nd quartz substage (3). Minor Ag-sulphosalts, tetrahedrite and base metal sulphides were also typically present. Wallrock alteration includes illite, kaolinite, passing outwards into I/S + kaolinite and smectite (Böhmer *et al.* 1969).

Low-angle second order vein structures join the 1st order fault on its western side. Veins in this position are less frequent, sometimes called the 3rd vein system. In the northern part, major groups of these veins are called Volle Henne. In the southern part these veins are antithetic, showing diagonal NNE-SSW strike and are called Katarína (Fig. 10). From the main fault structures they are separated by steep antithetic veins rich in Sb mineralization. The youngest are nearly perpendicular, W-E to NW-SE oriented veins (e.g. Křížne veins close to the Kremnické bane village) and are hosted in both andesite and rhyolite dykes.

South of Šturec, vein mineralization of the 1st vein system gradually wedges out. After about a 1.5 km break, vein mineralization reappears in the form of weakly mineralized quartz/chalcedony veins on the major N-S trending fault and continues about 3 km southward to the village Bartošova Lehôtka with average thickness 1 to 5 m. On the flat summit of the Čertov Vrch hill, ~3 km south from Šturec and 900 m west from the master fault, silicified hydrothermal breccias cemented by quartz/chalcedony with cinnabar are present, interpreted as a hot spring type mineralization (Veľký 1999). Surrounding rhyolite and rhyolite tuffs contain kaolinite, whereas south of the hill a deposit of the I/S mineral rectorite occurs (Kraus *et al.* 1994). It is likely that this hydrothermal system is connected to a weakly mineralised NE-SW trending structure, running under the W side of the plateau. Smectite-dominated alteration extends further S, associated with limnic/lacustrine silica deposits (fresh-water cherts and rare silica sinters).

The principal characteristics of the deposit are indicative of epithermal mineralisation of low sulphidation-style (Sillitoe & Hedenquist 2003): sericite (illite) and adularia are the key alteration minerals, mineralisation contains only minor base metal sulphides (including arsenopyrite), carbonate-replacement textures are typical, and main metals include only Au ± Ag.

New analytical data presented in this study have been obtained on samples from various sources: surface samples, samples from drill core material from various exploration campaigns during the last 15 years, historical samples from museums, archives and private collections. However, as the underground mines in Kremnica have already been closed for several decades, the samples obtained usually lack information about their position within the paragenetic

sequence published by Böhmer (1966) and Mat’o (1997). Fluid inclusion microthermometry was always accompanied by oxygen isotope study, which could be applied on much broader sample suite than the microthermometry.

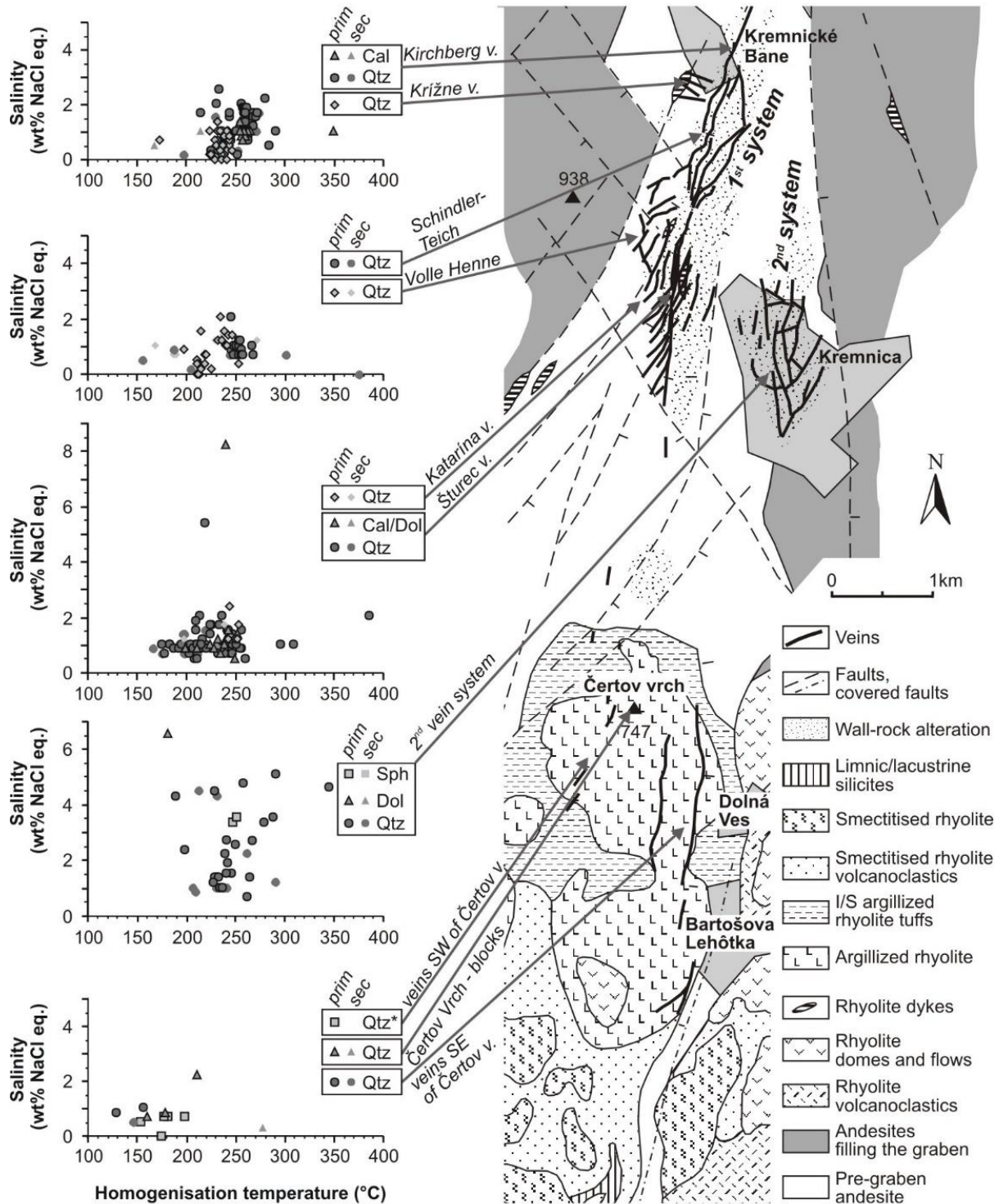


Figure 9. Structural scheme of the Kremnica hydrothermal system (modified from Kraus *et al.* 1994) with results of fluid inclusion microthermometry presented in series of homogenisation temperature vs. salinity diagrams for main segments of the system. *Data from Uhlík & Majzlan (2004).

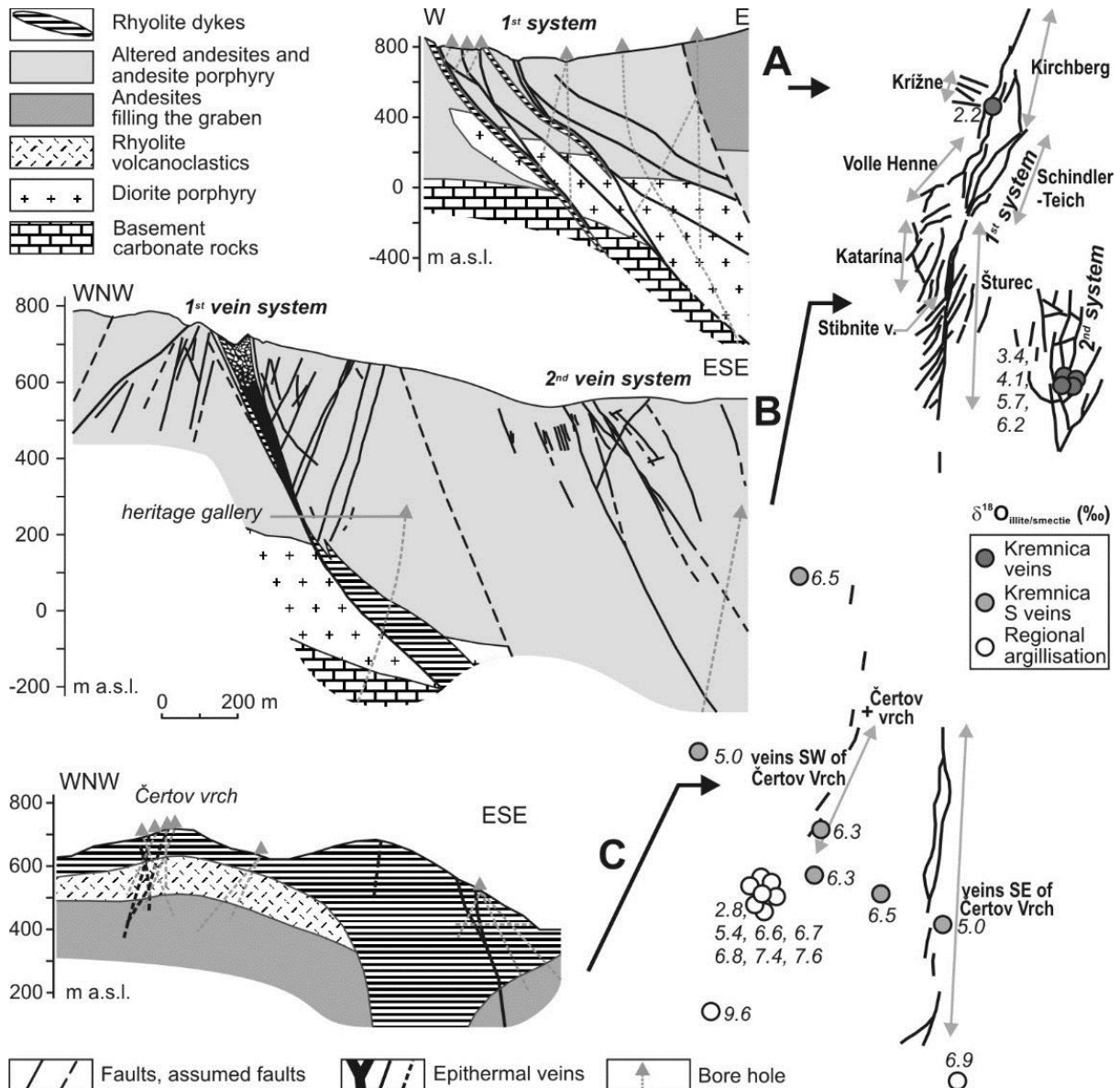


Figure 10. Schematic sections of northern (A), central (B) and southern (C) parts of the Kremnica Au-Ag deposit (after Böhmer & Škvarka 1970; Veľký *et al.* 1998) and scheme of vein systems with names for individual segments. Arrows point to approximate position of cross section lines. Also shown is location of samples of illite-smectite minerals with their oxygen isotopic composition values (in per mil).

5.2. Fluid inclusion data

Microthermometry was performed on inclusions in vein quartz, carbonate and sphalerite. According to their phase relationships at room temperature, two types of aqueous inclusion were recognized: two-phase liquid-rich and two-phase vapour-rich. Liquid-rich inclusions occasionally contain fibrous, birefringent minerals, which have never been observed to dissolve on heating, and are thus interpreted as captured phases (probably sericite). Vapour-rich inclusions commonly appeared to co-exist with liquid-rich inclusions, which is indicative of boiling during entrapment.

Microthermometric data are presented for individual parts of the ore field from N to S (Figs. 9, 11, Appendix 1). The northernmost part of the 1st vein system (Kirchberg) has the hottest fluid inclusion homogenisation temperatures, as measured from three underground samples that were collected from ~80 m, 170 m and 799 m depth (mean T_h values 259, 260 and 266°C). In contrast, a single surface sample showed a significantly cooler mean temperature of 236°C. Two surface samples from the structurally youngest Krížne veins showed similar T_h values (~235°C; Kovačič

2010) and they also contain evidence for boiling. There is a slight decrease in the mean T_h values from the neighbouring vein system segments Schindler-Teich (253°C from one underground quartz sample) and Volle-Henne (219°C from one surface sample), and the latter contains evidence of boiling.

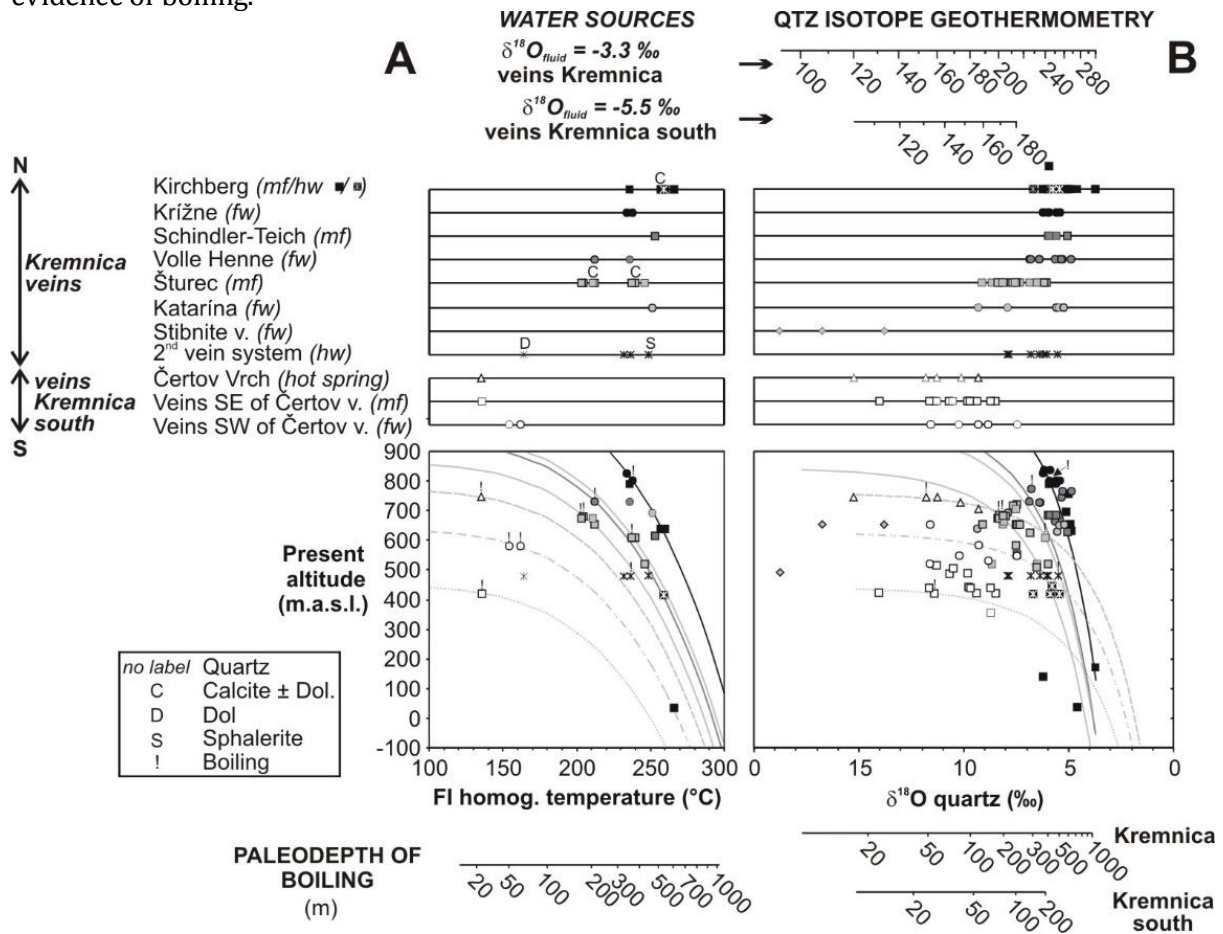


Figure 11. Comparative plots of analytical data on samples from the Kremnica Au-Ag deposit. (A) Summary of fluid inclusions homogenization temperatures (T_h), representing mean of the entire range of T_h values in individual vein samples (samples without boiling) or mean of the estimated boiling range for samples with evidence of boiling (Table 1). (B) Oxygen isotopic composition of vein quartz. Upper diagrams show summary of analytical data aligned on lines representing individual segments of the vein system (see Fig. 10). Also shown are ranges of equilibrium temperatures calculated for isotopic equilibrium with hydrothermal fluids (Zheng 1993). Note different temperature scales for Kremnica veins and for veins in Kremnica south due to different corresponding $\delta^{18}O_{fluid}$ values (see Fig. 12). Lower diagrams show T_h and $\delta^{18}O$ values plotted against present altitude of the analysed samples. Also shown are *boiling point for depth* curves (Haas 1971), fitted to cross the samples with evidence of boiling. At the bottom of the Figure ranges of paleodepth of boiling are shown, corresponding to hydrostatic pressure of boiling fluids with 1 wt % NaCl (Haas 1971). mf = master fault, hw = hanging wall faults, fw = footwall faults.

Most samples from the central part of the ore field (Šturec, Katarína and 2nd vein system veins) also showed two different sets of mean T_h values, depending on relative sample depth, and fluid inclusion populations commonly show evidence of boiling. Underground samples (~100 to 250 m) both from Šturec and Katarína veins had mean T_h values that mostly range from 239 to 251°C (3 samples), but one sample had a cooler mean T_h value of 211°C. Surface samples from the Šturec open pit also had cooler mean T_h values (~210°C). Due to a lack of available material, the 2nd vein system below the historical Kremnica townsite was studied just from two archived subsurface samples. One sample showed consistent mean T_h values of 232°C, but the other sample showed a broad range of T_h values (mean at 260°C for quartz, 249°C for sphalerite and 164°C for dolomite) and contains evidence for boiling and the presence of pure CO₂ in some vapor-rich fluid inclusions. However, the derivation of this sample from the 2nd vein system is not definite because it is an historical specimen.

Fine-grained quartz samples from the southern part of the ore field rarely contained inclusions that are suitable for microthermometry, but these rare inclusions commonly contain evidence for boiling. Fluid inclusions in a surface sample from a block of silica from the Čertov Vrch paleo-hot-spring system had a mean T_h value of 151°C. Two surface samples of veins located SW of Čertov Vrch both showed mean T_h values of ~178°C (Uhlík & Majzlan 2004). A sample of chalcedonic quartz SE of Čertov Vrch provided mean T_h value of 136°C.

Salinities of nearly all measured fluid inclusions were very low (<2 wt% NaCl eq.), which is typical for fluids associated with low sulphidation (adularia-sericite) epithermal systems (e.g. Simmons *et al.* 2005). Only inclusions from the 2nd vein system showed slightly increased salt contents that range from 0.7 to 6.6 wt% NaCl eq. (2.5 wt% in average), which could be related to intense boiling that formed bonanza-type gold accumulations. Due to the generally low salinities, eutectic temperatures (T_e) could be recorded only rarely. Even though a broad range of T_e values was measured (-21.7 to -49°C), most values occur in a narrow range from -33.5 to -39.4°C, which indicates a multicomponent fluids that probably contains FeCl₂ and MgCl₂ in addition to NaCl (Shepherd *et al.* 1985). Only a single sample from the 2nd vein system was observed to contain CO₂-bearing inclusions, and the melting of that CO₂ ranged from -56.5 to -57.1°C.

The variable T_h values observed among samples from same part of the hydrothermal system probably result from multiple stages of vein filling, as well as different depths for the samples. As is clear from Figure 11A, in individual vein segments deeper samples commonly show hotter average T_h values than those from higher altitude. Anomalously hot T_h values (> 290°C; Fig. 9) probably result from heterogeneous trapping of vapour and liquid in boiling fluid inclusion populations.

Evidence of boiling enabled calculation of paleopressures and paleodepths assuming hydrostatic pressures and low CO₂ content in fluids (Table 1). Only some parts of the vein system, mostly in the central and southern parts of the ore field, contain fluid inclusions that contain evidence of boiling fluids. The deepest paleodepths were determined in northern and central part of the deposit for the Krížne veins (320-420 m) and some samples from Šturec (330-410 m). Slightly shallower paleodepths are indicated for Volle Henne (200-220 m), and some Šturec samples (150-220 m), whereas the shallowest paleodepths (20 to 60 m) come from the southern part of the deposit.

Table 1. Summary of data from boiling fluid inclusion assemblages in vein quartz from various parts of the Kremnica ore field. Boiling pressure was determined from tables of boiling of NaCl-H₂O fluids (Haas 1976), depth of boiling was calculated for hydrostatic pressure in the same system (Haas 1971). *Data from Uhlík & Majzlan (2004)

Sample	Locality	T (°C)	Aver. salinity (wt% NaCl eq.)	P (bar)	Depth (m)
KB-4	Krížne	231-245	0.7	28-36	320-420
VH-4	Volle Henne	210-214	0.3	19-21	200-220
AS-4.2-97-101	Šturec	233-244	1.6	30-36	330-410
KŠ-2	Šturec	196-210	1.1	14-19	150-200
ST-1	Šturec	196-213	1.1	14-15	150-220
Pyr1	2 nd v. syst.?	231-242	2.7	28-34	310-390
Koper	Čertov vrch	130-141	0.8	3-4	20-30
BarLeh1	SE of Č. Vrch	128-142	0.9	3-4	20-30
DV-1	SW of Č. Vrch*	154	0.5	5	50
DDV-16	SW of Č. Vrch*	162	0.1	6	60

5.3. Stable isotope data

Monomineral separates from vein filling, wall-rock alteration and unaltered rhyolite were analyzed for their O, H and C isotope compositions (Appendixes 3 and 4) The $\delta^{18}\text{O}$ values of hydrothermal fluids coexisting with quartz and calcite and $\delta^{13}\text{C}$ of CO₂ in equilibrium with calcite were calculated using fractionation factors of Zheng (1993), Golishev (1981) and Ohmoto & Rye

(1979), respectively, applying temperatures derived from fluid inclusion microthermometry (Appendix 2). Oxygen and hydrogen isotopic composition of fluids in equilibrium with illite/smectite were calculated using equations of Sheppard & Gilg (1996) and Capuano (1992) using temperatures based on illite-smectite expandability (66 – 194°C, Appendix 3; Šucha *et al.* 1992; Harvey & Browne 2000). However, clay mineral geothermometry is affected by metastable behaviour of clays and is not based on equilibrium reactions (Essene & Peacor 1995), therefore the temperatures used can have an error ~30 to 60°C which in turn influences accuracy of calculated $\delta^{18}\text{O}_{\text{fluid}}$ values (up to 2-3 ‰) and $\delta\text{D}_{\text{fluid}}$ values (up to 10 ‰). Isotopic composition of fluids in equilibrium with biotite were estimated using equations of Bottinga & Javoy (1973) and Suzuoki & Epstein (1976) using assumed crystallization temperature 700°C and closure temperatures 540 and 430°C for O and H, respectively (Zaluski *et al.* 1994).

Oxygen isotope data of vein quartz from Kremnica veins show a similar pattern of spatial distribution of values as the fluid inclusion data (Fig. 11). In the northernmost part of the ore field, the deepest samples have the lowest $\delta^{18}\text{O}$ values in the entire field (down to 3.7 ‰), whereas shallower samples and more southerly located samples have higher values ranging from 4.9 to 9.3 ‰, correlating well with fluid inclusion homogenisation temperatures. Stibnite-rich veins at Šturec contained chalcedonic quartz with the highest $\delta^{18}\text{O}$ values in the entire field (13.8 to 18.8 ‰). $\delta^{18}\text{O}$ data from southernmost parts of the ore field are scattered in a broad range from 7.5 to 15.3 ‰, mostly with positive correlation with the altitude of analysed samples within the vein segments.

In some samples of vein quartz, hydrogen isotopes were analysed from fluid inclusions. The observed relatively broad range of values (-50 to -115 ‰ δD) does not appear to be related to position of samples within the ore field or depth of samples. Perhaps the relatively large variation results from extracting inclusion water accompanied by structural water, as discussed above (see Faure 2003).

Isotopic composition of fluids in equilibrium with quartz, carbonates, magmatic biotite and illite/smectite from samples of wall-rock alteration as well as regional alteration south and SE from the major vein system, are plotted in Figure 12. The major part of the Kremnica vein system shows a relatively narrow range of $\delta^{18}\text{O}_{\text{fluid}}$ values with median -3.3 ‰, but veins south of Kremnica have systematically lower $\delta^{18}\text{O}_{\text{fluid}}$ values with median -5.5 ‰. This difference might be related to different host rocks of both parts of the system (andesitic and rhyolitic) that are able to influence the composition of fluids by water-rock interaction. This might be the result either of different bulk $\delta^{18}\text{O}$ values of both rock types (not tested yet) or more likely due to their different hydrogeologic and mineral properties (greater permeability and reactivity of rhyolitic volcanoclastic rocks compared to andesites).

Relatively homogeneous but distinct oxygen isotopic signatures of hydrothermal fluids in Kremnica and Kremnica south vein districts enable estimation of equilibrium crystallisation temperatures for all samples with analysed $\delta^{18}\text{O}$ (Fig. 11), providing more detailed information on spatial temperature evolution of fluids than that available from fluid inclusion microthermometry. Oxygen isotope geothermometry based on quartz-water fractionation factor (Zheng 1993) assumes constant $\delta^{18}\text{O}$ fluid composition and thus provides only a rough estimate of quartz crystallisation temperatures.

The more scattered pattern of isotopic composition of fluids in equilibrium with I/S from regional alteration is probably related to uncertainty in their crystallisation temperatures, related to incomplete water-rock interaction during their origin (Harvey & Browne 2000). Magmatic biotite from unaltered rhyolite showed low $\delta\text{D}_{\text{fluid}}$ values that can be interpreted to result from isotopic fractionation during exsolution of fluid from crystallising magma in an open system (Taylor 1997). However, generally relatively low $\delta^{18}\text{O}$ values of fluids in the Kremnica hydrothermal systems indicate a predominant meteoric water source in the fluids, albeit affected by fluid-rock interaction resulting in $\delta^{18}\text{O}$ shift from the meteoric water line; this is typical for low sulphidation epithermal systems (Cooke & Simmons 2000).

The isotopic composition of kaolinite from vein wall-rock alteration (5.5 to 10.2 ‰ $\delta^{18}\text{O}$, -79 to -92 ‰ δD) is indicative of a steam-heated origin at 50-90°C (Sheppard & Gilg 1996). It is

interpreted to result from a collapse of acid sub-surface waters down into the system during final stages of mineralisation.

Carbon isotopic compositions of vein carbonates (-1.1 to -4.4 ‰ $\delta^{13}\text{C}_{\text{CO}_2}$) are typical of carbonates from epithermal deposits (Field & Fifarek 1985). Application of quartz-calcite oxygen isotope geothermometry (Sharp & Kirschner 1994) provided a temperature 217°C for the Šturec quarry, corresponding well with the results of fluid inclusion microthermometry.

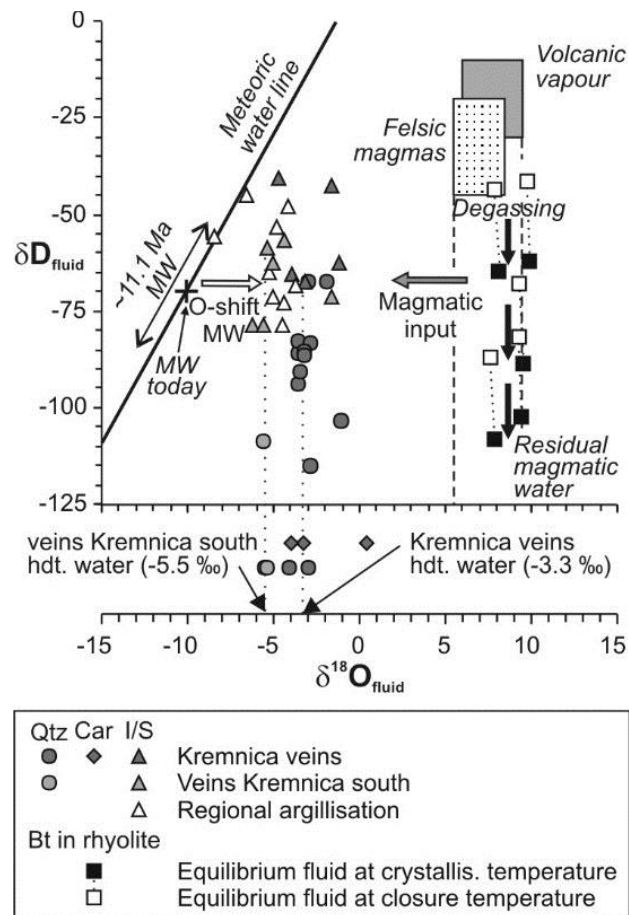


Figure 12. Isotopic composition of water in equilibrium with minerals from vein filling, regional alteration and rhyolite in the Kremnica hydrothermal system. See Figure 7 for explanation of arrows and related references. Composition of MW during the origin of epithermal mineralization is reconstructed based on paleoclimate information. Low δD values of fluids in equilibrium with biotite phenocrysts are probably the result of open system degassing in parental magma chamber, whereas δD values of fluids in equilibrium with quartz may result from problems of extraction of water from fluid inclusions (Faure 2003). Highlighted by thin arrows are mean $\delta^{18}\text{O}_{\text{fluid}}$ values in equilibrium with Kremnica veins and veins in Kremnica south calculated at temperatures based on fluid inclusion microthermometry.

5.4. Genetic model

New data on fluid properties of the Kremnica hydrothermal system enabled us to reconstruct the history of spatial and temporal fluid evolution, including estimates of erosion level of individual parts of the vein system (Table 2). Erosion level could be determined from hydrostatic pressure of boiling fluids or from minimum pressures (in case of vein system segments with no evidence of boiling), assuming pressure conditions greater than those necessary for boiling. Erosion estimate data show decreasing erosion level from north to south of the master fault veins (1st vein system) from >350 m to <100 m. The different erosion levels are most likely related to stepwise synmineralization uplift of the resurgent horst, that was most intensive in northern part of the deposit. Erosion level estimates are also in agreement with the geological evidence of different uplift of veins in the footwall and hanging wall of the master fault, which are also arranged in stepwise manner with the lowest uplift/erosion on hanging-wall veins closest to the

margin of the horst (100-310 m) and highest uplift/erosion on the footwall veins (320-500 m; Table 2, Fig. 10). Broad or multiple ranges of paleodepths of boiling and erosion level within individual vein segments are related to the presence of multiple stages of mineralisation coeval with the subsequent horst uplift. The significantly lower erosion level of the southern part of the ore field is consistent with preservation of rhyolitic rocks overlying andesite in this part of the hydrothermal system.

Table 2. Summary of main characteristics of individual parts of the Kremnica ore field. Paleodepth of boiling was calculated for hydrostatic pressure in the system NaCl-H₂O (Haas 1971), based on data on boiling fluid inclusion assemblages presented in Table 1. For vein system segments with no evidence of boiling, minimum paleodepth of boiling was estimated assuming fluid pressures higher than those necessary for boiling. Erosion level estimate is based on data on paleodepth of boiling and present position of analysed samples with respect to vein outcrops on surface (Fig. 11). See text for interpretations.

Locality	Position of host structures	Elevation of vein outcrop (m.a.s.l.)	Paleodepth of boiling (m)	Erosion level estimate (m)
Kirchberg main veins	master fault			
Kirchberg hanging wall v.	hanging wall faults	780-820	>350	350-500
Křížne	footwall faults	700-730	>410	100-240
Schindler-Teich	master fault	790-850	320-420	320-500
Volle Henne	footwall faults	725-735	>410	370-470
Šturec	master fault	730-770	200-220, >450	~210, 320-350
Katarína	footwall faults	665-760	150-220, 330-410	150-220, 250-275
Šturec Sb veins	footwall faults	720-750	>450	360-460
2 nd vein system	hanging wall faults	700-720	Above boiling level	Not applicable
Čertov vrch	paleohot-spring system	530-590	310-390	110-310
veins SW of Čertov v.	system	730-745	20-30	10-30
veins SE of Čertov v.	footwall faults	550-670	50-60	25-100
	master fault	420-525	20-30	10-70

The Kremnica ore field is a typical low sulphidation epithermal system in a specific high relief terrain setting (Fig. 13), whereas classic genetic models of this deposit type are developed mostly for low relief terrain (e.g. Sillitoe & Hedenquist 2003). Even today, the vertical difference between northern and southern ends of the Kremnica vein system is about 450 m.

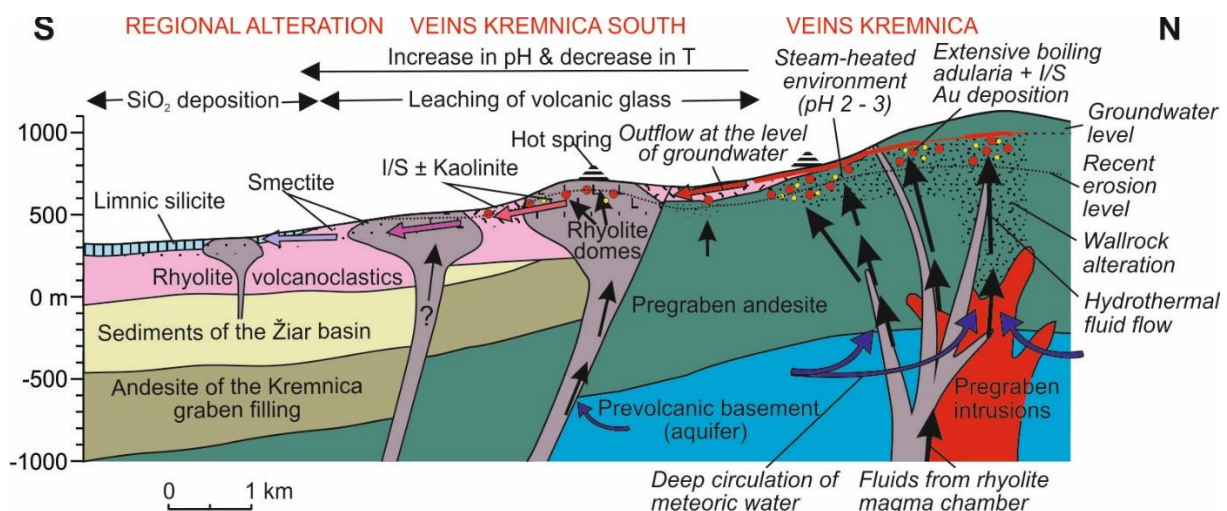


Figure 13. Schematic model of the Kremnica hydrothermal system, drawn as a N-S cross section along the Kremnica vein system and associated regional alteration (after Koděra & Lexa 2010).

Stable isotope data indicate isotopically homogeneous sources of fluids: deeply-circulating, mostly meteoric, waters, driven by heat from the contemporaneous rhyolite magma chamber. Low salinities indicate only a minor magmatic component in the fluids, which is typical for low sulphidation epithermal systems (~10 %; Cooke & Simmons 2000). However, more significant

involvement of low salinity magmatic fluids, such as condensed magmatic vapour neutralised at depth cannot be entirely excluded (Sillitoe & Hedenquist 2003; Heinrich 2005). Basement rocks including permeable carbonates (Fig. 10) probably served as aquifers for development of large convection cells, drained by fault structures associated with the horst uplift. Decrease in pressure of ascending hydrothermal fluids resulted in boiling accompanied by low-sulfidation style of alteration and precipitation of gold due to escape of vapour and decomposition of dissolved Au complexes (Hedenquist *et al.* 2000). The complex system of hydrothermal veins with multiple stages of mineralization is consistent with a long-lived hydrothermal system.

Widespread presence of kaolinite in veins and in the wall rock indicates formation of large areas of steam-heated waters that probably accompanied the veins at subsurface level. Acid alteration resulted from condensation of H₂S and CO₂-bearing vapour released during boiling (Hedenquist & Arribas 1999; Simmons *et al.* 2005). During later stages, these acid steam-heated waters were able to collapse into host structures, overprinting earlier low-sulphidation alteration assemblages (e.g. Reyes 1990; Simpson *et al.* 2001).

Feeder faults terminating in permeable rhyolite volcanoclastic rocks rich in volcanic glass could be responsible for the extensive regional-scale I/S and smectite alteration (including K-bentonite and bentonite deposits), which affects only rhyolitic rocks in the area south of the Kremnica horst. Flow of hydrothermal fluids in permeable rocks at subsurface levels was driven by decreasing hydraulic head, i.e. mostly to south and SE direction, with local discharge on paleosurfaces (e.g. Čertov Vrch hot spring system). Migrating fluids were able to decompose volcanic glass in rhyolitic rocks forming clays whereas fluids became enriched in SiO₂, progressively cooler, and of more neutral pH (Sillitoe 1993). Upon reaching the local limnic/lacustrine basins the fluids discharged SiO₂ creating limnic silica deposits, alternating with sedimentation of reworked tuffs later converted to clays (bentonite).

6. Au-mineralization at the Javorie stratovolcano

Javorie stratovolcano is a large compound stratovolcano involving a volcanotectonic graben and subvolcanic intrusive complex that evolved in several stages of volcanic/magmatic activity during Middle Miocene, roughly in the interval 15.0 to 11.0 Ma (Konečný *et al.* 1998a). The pre-graben stage gave rise to a large andesite stratovolcano. Following a period of denudation, subsidence of the volcanotectonic graben in the central zone of the stratovolcano took place. This was accompanied at first by effusive activity of basalts and mafic andesites, and later by activity of amphibole-pyroxene andesites to dacites giving rise to a number of extrusive domes. Emplacement of andesite porphyry, quartz-diorite porphyry and monsofordiorite stocks (Kalinka and Kráľová intrusive complexes) into subsided complexes of the graben filling were accompanied by evolution of magmatic-hydrothermal systems (including Au-porphyry mineralization). Based on succession and biostratigraphic evidence (Konečný *et al.* 1998a) their age should be around 13.0 Ma. During the post-graben stage, renewed andesite activity formed an extensive stratovolcanic complex of the Javorie Formation (Fig. 2).

Centres of magmatic-hydrothermal activity correspond to areas of strong hydrothermal alteration with barren zones of advanced argillic alteration. Recent exploration has discovered the presence of Au-porphyry mineralization in 7 hydrothermal centres (Hanes *et al.* 2010), but only one locality represents an economic accumulation of ore – the Biely Vrch deposit (44 Mt @ 0.98 ppm Au, www.emed-slovakia.com). All systems are centred on small diorite to andesite porphyry stocks up to 1-1.5 km in diameter emplaced into andesites of the pre-graben stage.

6.1. Au-porphyry mineralization

The Biely Vrch Au deposit is hosted by the northernmost magmatic-hydrothermal system located in a relatively shallow NE part of the volcanotectonic graben. The deposit is centred on a biotite-amphibole diorite to andesite porphyry stock 300x400 m in extent, emplaced into andesites of the pre-graben stage, and in the deeper level granodiorite/tonalite of the Hercynian

basement found in blocks in some exploration drill holes. Post-mineralization andesites and epiclastic breccias of the Javorie Fm. occur south and east of the deposit (Hanes *et al.* 2010, Koděra *et al.* 2010a). Mineralization extends from surface to a depth of at least 700 m (Fig. 14).

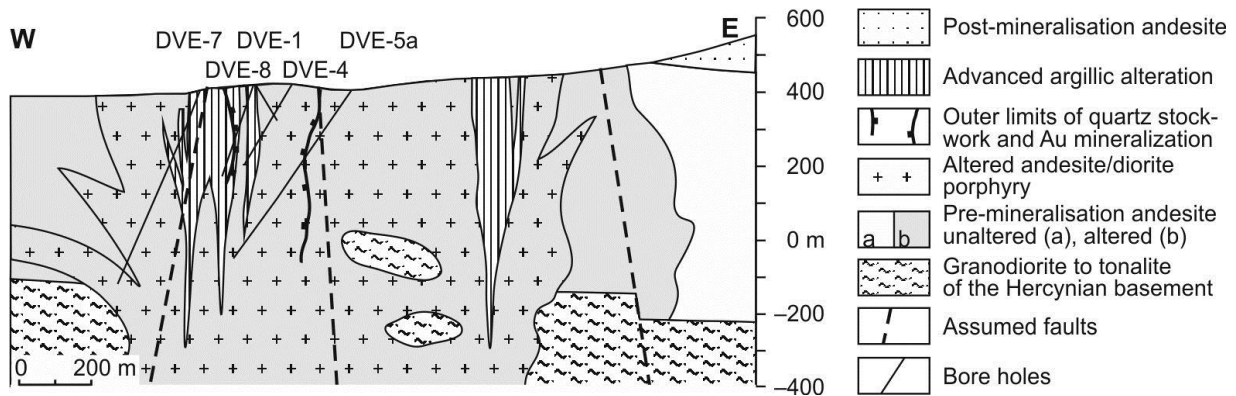


Figure 14. Schematic geological section of the Biely Vrch Au-porphyry deposit (after Koděra *et al.* 2010a).

The porphyry stock and surrounding andesite and epiclastic breccias are affected by extensive alteration (Koděra *et al.* 2010a). Intermediate argillic alteration dominates, represented mostly by illite-smectite, illite, chlorite and pyrite, and variably overprints earlier high-temperature K-silicate (K-feldspar, biotite, magnetite/pyrrhotite) and Ca-Na silicate (intermediate to basic plagioclase, actinolite) alteration at deeper levels of the system. Propylitic alteration (illite-smectite, chlorite-smectite, chlorite, pyrite) affects the outer zone of the system. Ledges of advanced argillic alteration (kaolinite, dickite, pyrophyllite, alunite, vuggy quartz) represent the youngest stage of alteration, most probably related to a younger intrusion at depth.

Alteration is accompanied by several generations of hydrothermal-explosive breccias and veinlets (Koděra *et al.* 2010a). These include earliest biotite-magnetite veinlets associated with K-silicate alteration and several generations of widespread quartz veinlets including A-type (quartz ± biotite or chlorite) and later banded quartz, with banding resulting from high content of vapour-rich fluid inclusions and micrometer-sized magnetite and ilmenite grains (Fig. 15 a). Botryoidal textures are continuous across quartz grains, suggesting recrystallization from silica gel. Rare veinlets of sulphides (pyrite, chalcopyrite ± magnetite, marcasite, galena, sphalerite), accompanied mainly by chlorite and illite-smectite, are related to intermediate argillic alteration. Late carbonate-zeolite veinlets are also relatively common. Veinlets with kaolinite, pyrophyllite and aluminum phosphate-sulfate minerals accompany ledges of advanced argillic alteration.

Stockwork of quartz veinlets marks the area of economic Au mineralization with very low Cu/Au ratio (0.018 wt% Cu/ppm Au; Hanes *et al.* 2010). Small gold grains of high fineness occur next to quartz veinlets in altered rock with clays, chlorite and K-feldspar, occasionally attached to sulphides or Fe-Ti oxides. Gold of the highest fineness is associated with advanced argillic alteration; however, ledges of advanced argillic alteration are mostly barren, except where they overprint mineralised quartz veinlets.

6.2. Fluid inclusion data

Preliminary fluid inclusion study was performed on a sample suite of vein quartz, representing various types of veins from various depths down to 440 m (Appendix 4). Visible liquid-absent vapour-rich fluid inclusions (type V) dominate in all generations of vein quartz (Fig. 15 b). They are clearly of multiple generations and in most samples account for >95% of all inclusions (Koděra *et al.* 2011). Some quartz veinlets (especially A-type) also locally host inclusions containing several salt crystals dominated by a green anisotropic solid and a distorted vapor bubble in mostly constant phase proportions, but with no visible aqueous liquid (type S; Fig. 15 c). Sometimes tiny opaque minerals are also present here (mostly magnetite and chalcopyrite). Based on analytical data (see below), these inclusions are interpreted to represent salt melts, heterogeneously trapped with coexisting vapour. Rarer, vapour-free, salt melt inclusions with tiny opaque grains

are also occasionally associated, possibly due to metastability or necking down of inclusions. Liquid-rich inclusions, in rare cases containing a small halite daughter crystal (type L), are present only rarely and are usually secondary in origin or associated with late generations of vein quartz.

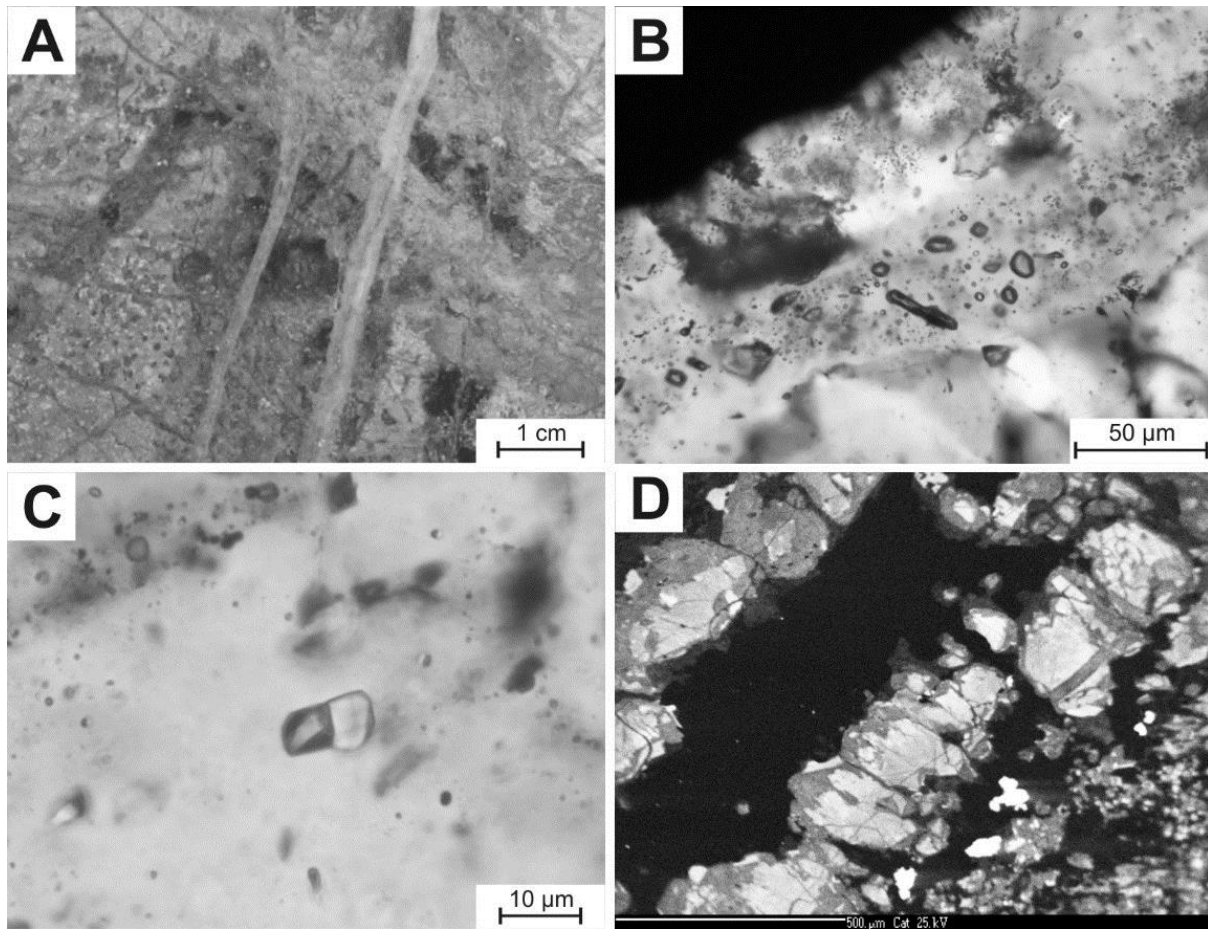


Figure 15. Images from the Biely Vrch Au-porphyry deposit: (A) Several generations of quartz veinlets in heavily silicified and argillised porphyry. (B) Detail of a banded quartz veinlet with a band rich in vapour-rich type of inclusions. (C) Typical inclusion with salt melt and vapour, hosted in the early A-type vein quartz. (D) SEM-CL image of the central part of an A-type vein. The bright luminescent quartz is replaced by dull luminescent quartz along grain boundaries and crosscutting veins. Central part of the vein contains pyrite (black).

Cathodoluminescence imaging of quartz stockwork showed complex structure of veinlets, with earliest A-type veinlets having strongest luminescence and being host to salt-melt bearing inclusions, whereas the latest banded veinlets show the weakest luminescence and host numerous small vapour inclusions, tiny magnetite grains and rare liquid-rich inclusions. Quartz in earliest veinlets was locally found to host silicate melt inclusions and therefore the temperature of crystallisation is probably close to that of groundmass of the porphyry intrusion. Based on the Ti-in-quartz geothermometer (Thomas *et al.* 2010), calibrated for growth rate and changing activity of TiO_2 with temperature (Koděra *et al.* 2013), early quartz veins started to form at $\sim 700\text{-}720^\circ\text{C}$ (247-284 ppm Ti), but the majority of the A-type veins precipitated between 650 and 590°C (104-168 ppm Ti). Subsequent cooling is associated with decreasing amounts of precipitating quartz with a minimum at 460 to 380°C (8-23 ppm Ti). Local resorption of early quartz grains (Fig. 15 d) has been observed, which is consistent with retrograde solubility of quartz during isobaric cooling from ~ 500 to 400°C below ~ 0.3 kb (Fournier 1995; 1999; Müller *et al.* 2010). A greater proportion of vein quartz, including banded veinlets, precipitated or re-crystallized from gel again below 380°C (detection limit of Ti) due to oversaturation of SiO_2 on cooling (Muntean & Einaudi 2000).

Due to low density of vapour-rich inclusions it was not possible to measure any phase changes in them, except for a single inclusion containing CO_2 . Microthermometric measurements on

inclusions with salt melts showed quick melting of the solids in the range 321-361°C (mostly 321-333°C), but total homogenisation was never reached prior to 850°C, indicative of diffusion of H₂O out of the inclusions (Doppler *et al.* 2013), heterogeneous trapping and/or post-entrapment modification due to α - to β -quartz transition upon cooling and reheating. The fluid properties of liquid-rich inclusions hosted in quartz (salinity 0.5-30.4 wt% NaCl eq. - mostly 1-5 wt% NaCl eq., T_h 191-269°C) suggest trapping from late fluids (Fig. 16), probably related to intermediate and advanced argillic alteration (Žitňan, 2010). Variable eutectic temperatures (-58 to -22°C) suggest the presence of different chemical systems, including NaCl-CaCl₂-H₂O. Primary fluid inclusions in vein calcite had salinity approaching 0 wt% NaCl eq. and homogenization temperature in range 131 to 242°C.

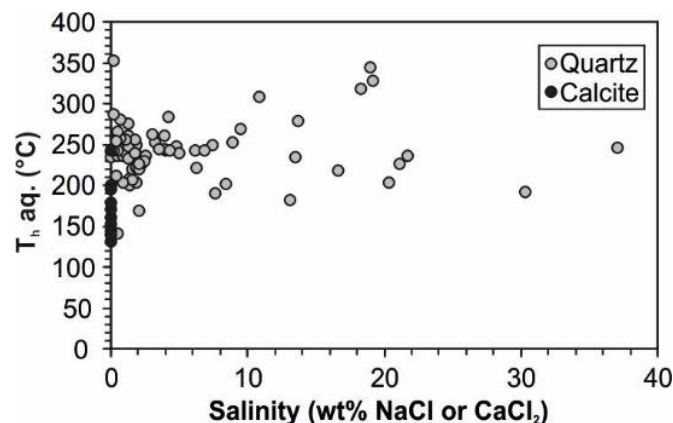


Figure 16. Homogenization temperatures (T_h aq.) versus salinity diagram of rare, mostly secondary liquid-rich fluid inclusions in various samples of vein quartz and calcite from the Biely Vrch Au-porphyry deposit.

Preliminary laser-ablation ICPMS microanalysis performed at the Department of Earth Sciences at ETH Zürich was used to quantify the composition of major and trace elements in the salt melt-bearing and vapour inclusions (Koděra *et al.* 2011). Microanalysis showed that salt melts contain Fe-K-Na-Cl in relatively stable proportions (FeCl₂>KCl>NaCl). Data from vapour-rich inclusions showed very similar Fe-K-Na-Cl proportions as those in salt melt bearing inclusions. High Fe concentration of the fluids is probably related to the dioritic composition of the parental melt. Experimental work of Zajacz *et al.* (2012) showed that for andesitic melts in upper crustal magma chambers, K and Fe partition more strongly into Cl-bearing volatiles (relative to Na) compared to felsic systems. In several populations of vapour-rich and salt melt-bearing inclusions, both Au and Cu were detected but not quantified due to a lack of information on their total salinity. Compared to the average Cu/Au ratio of the deposit, most of the inclusion populations had similar or even lower Cu/Au ratio. In respect to total salinity of inclusions, gold is preferentially concentrated in vapour, which points to the major type of fluid introducing gold in the porphyry system. Cu and Ag do not show preferential concentration.

Low density vapour, accompanied by extreme “brines” found in fluid inclusions in quartz veinlets, resulted from fluid heterogenisation at very low pressures (<0.3 kbar) which can be deduced from phase relations in the system NaCl-H₂O (e.g. Williams-Jones & Heinrich 2005). According to the phase relations in this system at such conditions, the fluids have reached the vapour+liquid+halite surface forming anhydrous salt melts in addition to a much bigger volume of vapour. This is in contrast to classical Cu-porphyry systems where fluid heterogenisation at greater pressures results in formation of saline brines (and vapour), precipitating daughter minerals in fluid inclusions upon cooling.

The obtained data on temperature evolution of fluids correspond well to evolution of the classic Au-porphyry systems in the Maricunga belt (Muntean & Einaudi 2001), where early A-type veinlets originated at 720-620°C and latest banded veinlets at 380-200°C with continuous decrease in temperature and pressure.

6.3. Stable isotope data

Vein minerals, alteration minerals and magmatic phenocrysts were analyzed for their O, H and S isotope compositions (as appropriate) (Koděra *et al.* 2011; Appendixes 5 and 6). Isotopic composition of vein quartz was analysed from 33 samples from various depths (72-780 m); however, the observed variation of $\delta^{18}\text{O}$ was very small (mean 9.4 ‰, standard deviation 0.7) and not related to depth (Fig. 17). Seven analyses of $\delta^{18}\text{O}$ of magnetite from host-rock alteration (90-572 m) also showed only minor variation (2.6 ± 0.6 ‰). Assuming isotopic equilibrium of quartz and magnetite with the same fluid, quartz-magnetite isotope geothermometry yields 595°C (Zheng & Simon 1991) or 680°C (Clayton & Keiffer 1991). At these temperatures mean isotopic composition of equilibrium fluids would be 7.4 or 8.0 ‰ $\delta^{18}\text{O}$ (Hu & Clayton 2003), which are values consistent with high temperature magmatic vapour as the major source of fluids (Fig. 17).

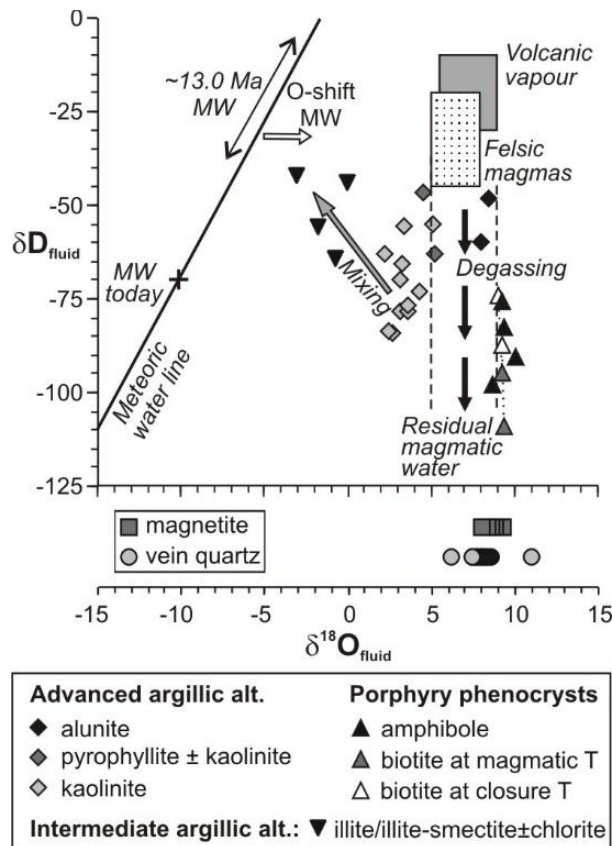


Figure 17. Isotopic composition of fluids in equilibrium with magmatic minerals, alteration minerals and quartz veinlets from the Biely Vrch Au-porphyry deposit. Composition of MW during the origin of porphyry mineralization is reconstructed based on paleoclimate information. See Figures 7 and 12 for explanation of arrows and related references.

Oxygen and hydrogen isotopic composition of fluids in equilibrium with other alteration minerals were calculated using equations of Stoffregen *et al.* (1994 – alunite O,H), Savin & Lee (1988 – pyrophyllite O), Sheppard & Gilg (1996 – pyrophyllite H, illite/smectite O,H), Gilg & Sheppard (1996 – kaolinite H) and Capuano (1992 – illite-smectite H). Fluids in equilibrium with alunite and pyrophyllite from ledges of advanced argillic alteration (youngest stage of alteration) indicate mainly a magmatic source (4.5 to 8.4 ‰ $\delta^{18}\text{O}_{\text{fluid}}$, -46 to -63 ‰ $\delta\text{D}_{\text{fluid}}$). A crystallization temperature for coarse-grained alunite of 294°C was estimated using oxygen isotope fractionation between SO_4 and OH groups (Stoffregen *et al.* 1994). Sulphur isotope data for alunite ($\delta^{34}\text{S}$ 10.6 to 15.6 ‰) are suggestive of a magmatic-hydrothermal origin for the S. Fluids in equilibrium with kaolinite, calculated at 200°C, show progressive but minor mixing with meteoric water (2.1 to 5.1 ‰ $\delta^{18}\text{O}_{\text{fluid}}$, -55 to -84 ‰ $\delta\text{D}_{\text{fluid}}$). Fluids in equilibrium with illite-smectite or illite from intermediate argillic alteration were calculated at temperatures based on illite-smectite expandability (142 – 187°C; Šucha *et al.* 1992; Harvey & Browne 2000). However, clay mineral geothermometry is affected by metastable behaviour of clays and is not based on equilibrium

reactions (Essene & Peacor 1995), therefore the temperatures used can have an error ~ 30 to 60°C which in turn influences accuracy of calculated $\delta^{18}\text{O}_{\text{fluid}}$ values (up to 2.6 ‰) and $\delta\text{D}_{\text{fluid}}$ values (up to 10 ‰). The obtained values (-3.0 to 0.0 ‰ $\delta^{18}\text{O}_{\text{fluid}}$; -42 to -65 ‰ $\delta\text{D}_{\text{fluid}}$) are indicative of mixing of magmatic and meteoric water fluids, because the intermediate argillic alteration data shown on Figure 17 lie in a field between the “felsic magmas” box and the meteoric water line. The data are roughly aligned towards the isotopically heavy region of the meteoric water line, which is consistent with the isotopic composition of meteoric water during the emplacement of parental diorite porphyry intrusion, influenced by humid subtropical climate (Planderová *et al.* 1993). However, hydrothermal fluid composition was probably also influenced by water-rock interactions resulting in O-shift away from the meteoric water line.

Fluids in equilibrium with biotite and amphibole from deep unaltered porphyry ($> 700\text{m}$) were calculated using equations of Bottinga & Javoy (1973) and Suzuoki & Epstein (1976), applying crystallization temperature 710°C and biotite closure temperatures 540 and 430°C for O and H, respectively (Zaluski *et al.* 1994). Equilibrium fluids showed a clear magmatic signature with low $\delta\text{D}_{\text{fluid}}$ values (-98 to -73 ‰) suggestive of isotopic fractionation during open system magma degassing (Taylor 1997).

6.4. Genetic model

The Biely Vrch deposit is a typical Au-porphyry system, displaying all major characteristics observed worldwide for this type of porphyry deposit, including very low Cu/Au ratio, association with diorite porphyry intrusions, enrichment in magnetite and presence of banded quartz veinlets (Seedorf *et al.* 2005). Au-porphyry systems are thought to represent the most shallow group of porphyry deposits (< 1 km; Muntean & Einaudi 2000; 2001) with strong consequences for fluid properties. Paleovolcanic reconstruction indicates that porphyry intrusions at Biely Vrch were emplaced at a depth of about 500 m below the paleosurface (Konečný *et al.* 1998a). Shallow emplacement of the parental intrusion is also suggested by unusual fluid inclusion properties of early magmatic fluids, where liquid-absent extremely saline brines (salt melts) accompanying dominant vapour are the result of fluid heterogenisation at very low pressures and high temperatures. Strong changes in SiO_2 solubility observed by resorption of early vein quartz and botryoidal textures of late banded veinlets are also typical for magmatic-hydrothermal systems cooling in low pressure environments (Fournier 1985). Furthermore, a high degree of telescoping of later alteration, down to the level of the Ca-Na silicate zone, is also consistent with the shallow level of the magmatic-hydrothermal system.

According to the preliminary genetic model (Fig. 18), a stockwork of quartz veinlets that mark the area of economic Au mineralization, has started to develop shortly after emplacement of the parental intrusion, from a magma saturated in water (stage 1). High temperature magmatic fluids are also responsible for early alteration patterns in a zonal arrangement (potassic, sodic-calcic, propylitic). Early advanced argillic alteration developed close to the surface due to condensation of magmatic gases rich in acid-forming components (mainly SO_2). Andesite magma of the parental intrusion was a crystal mush of biotite, amphibole, plagioclase and quartz phenocrysts in a highly differentiated melt of rhyolitic composition with a high water content (6.5 - 7.2 wt%), and evolved in a lower crustal magma chamber at pressures 5.5 - 8 kbar and $\sim 700^\circ\text{C}$ (Lexa *et al.* 2012; Koděra *et al.* 2013). However, the dacite melt water saturated solidus (Holtz *et al.* 2001) implies that the Biely Vrch diorite porphyry emplacement was at a temperature $\sim 850^\circ\text{C}$. This temperature, and reaction coronas of biotite and amphibole phenocrysts, constrain PT conditions of the parental shallow magma chamber to values $\sim 850^\circ\text{C}$ and $< 1 - 1.5$ kbar (Holtz *et al.* 2005; Blundy *et al.* 2006). Hotter temperature of magma in the high-level chamber than in the deep magma reservoir indicates that mafic magma was probably injected into a cooler and more felsic deep magma chamber below Biely Vrch.

After solidification of the apical part of the intrusions and during cooling of the system, continuous escape of magmatic fluids from depth has further mineralised the network of veinlets and cracks down to mesothermal temperatures (stage 2). Gold was introduced to the system probably mostly by magmatic vapour as indicated by the LA/ICPMS data. Most Au was probably

precipitated as a result of extreme phase separation, together with feldspar and Fe-oxides, but without abundant sulphides, due to the effective stripping of the stabilising hydration sphere of gold complexes in a high-temperature but low-pressure subvolcanic fumarole environment (Williams-Jones & Heinrich 2005). The presence of transitional quartz-sericite-pyrite (phyllic) alteration is assumed to have likely occurred below the advanced argillic lithocap (e.g. Sillitoe 2010), but is probably not preserved today.

Further cooling of the system (stage 3) is related to initial meteoric water incursion and development of widespread intermediate argillic alteration that overprints earlier alteration patterns. Based on fluid inclusion and stable isotope data, this alteration is associated with cooler (< 270°C), nearly neutral pH fluids, probably with only a minor magmatic component. During this stage, significant paleosurface degradation is assumed to have occurred, especially of the soft argillised material.

The final, fourth stage of the model corresponds to the origin of zones and ledges of advanced argillic alteration that generally result from condensation of magmatic vapour enriched in acidic volatiles, starting at temperatures >300°C and later mixing with meteoric water (Sillitoe 2003). These fluids were likely related to a new portion of magma emplaced at depth.

In the clay mineral stability field, partial remobilisation of gold has probably taken place by late aqueous fluids, as indicated by several generations of gold with different fineness. Introduction of new gold to the system by fluids associated with advanced argillic alteration is unlikely, as this alteration contains gold only where spatially overlapping with earlier quartz stockwork. Furthermore, at other localities within the Javorie stratovolcano this type of alteration is mostly barren (Hanes *et al.* 2010).

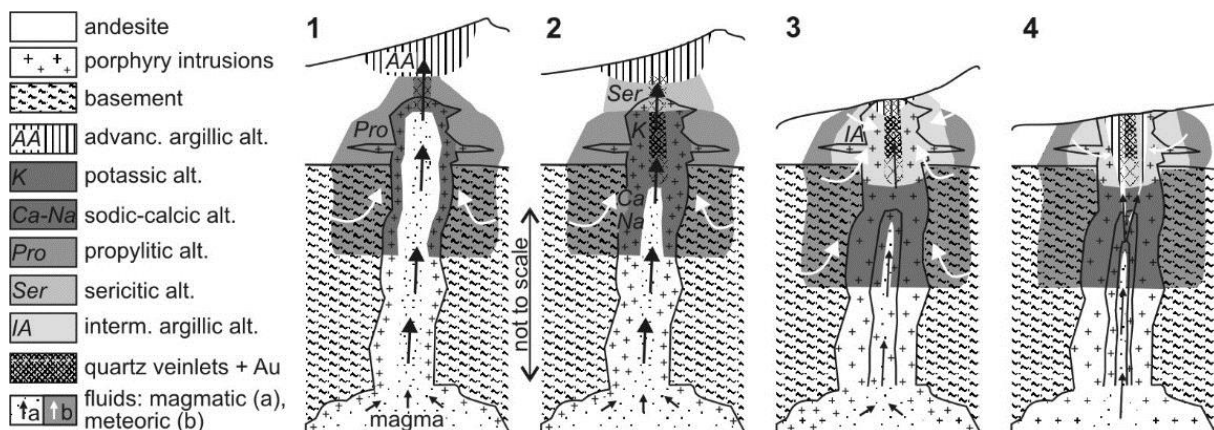


Figure 18. Genetic model of the Biely Vrch Au-porphyry deposit with schematic succession of magmatic and hydrothermal activities, alteration patterns and mineralization (modified from Koděra *et al.* 2010a).

7. Conclusions

The Central Slovakia Volcanic Field hosts various types of economic gold mineralization, related to magmatic-hydrothermal activity in central zones of large andesite stratovolcanoes, including intermediate sulphidation, low sulphidation, and porphyry deposits. Fluid inclusion and stable isotope research provided essential data to determine fluid properties, fluid sources and probable triggers for Au precipitation. Each of the three systems described in this paper has a very specific geological and structural position in stratovolcanic edifices and is related to different types of magmatism, which largely influenced fluid properties of the corresponding hydrothermal system.

Rozália Au-Ag deposit is a specific intermediate sulphidation epithermal system, influenced by development of subhorizontal structures related to a caldera-collapse stress field. Mixed magmatic and meteoric fluids had as the source of heat and magmatic components a shallow differentiated magma chamber at the base of the volcano, which was also responsible for the emplacement of nearly coeval quartz-diorite porphyry sills. Precipitation of gold occurred

because of prolonged boiling induced by pressure decrease and transition from suprahydrostatic to hydrodynamic conditions.

Kremnica Au-Ag deposit is a typical low sulphidation epithermal system, contemporaneous with rhyolite magmatism and uplift of a resurgent horst during the final stages of volcanic evolution. Dominantly meteoric fluids with probably a minor magmatic component were driven by heat of the parental rhyolite magma chamber and released gold because of extensive boiling. The specific setting of the system, in a high relief terrain with changing erosion level, is responsible for the observed gradual decrease in fluid temperature along the vein system.

Au-porphyry deposit Biely Vrch is a typical intrusion-related system with dominant participation of high temperature magmatic fluids, introduced by a highly differentiated andesitic magma emplaced at a very shallow depth at high temperature. Low density magmatic vapour was here the major source of gold, which precipitated in a high-temperature but low-pressure subvolcanic fumarole environment.

The developed genetic models for different Au-bearing deposits within one volcanic field can be used to guide exploration not only in this district but also in other regions worldwide with a similar magmatic-hydrothermal and structural history.

Acknowledgements

This study was supported by the Slovak Research and Development Agency, contract No. 0537-10, by VEGA grants 1/0311/08, 2/0171/08 and 2/0162/11, by projects 0801-840-302/160, ZP-547-010, 0503 and 1506 financed by the Ministry of Environment of the Slovak Republic and by IGCP project 540. Assistance was provided by EMED Mining, Ltd., Slovenská Banská s.r.o. and Tournigan Gold Corporation. Work at SUERC was supported by funds derived from NERC and the Scottish Universities. We thank Jeffrey L. Mauk for his constructive review, which has helped to improve the manuscript.

References

- Bakos, F., Chovan, M., Bačo, P., Bahna, B., Ferenc, Š., Hvožd'ara, P., Jeleň, S., Kamhalová, M., Kaňa, R., Knésl, J., Krasnec, Ľ, Križáni, I., Maťo, Ľ., Mikuš, T., Paudits, P., Sombathy, L. & Šály, J. 2004. Gold in Slovakia. Slovenský skauting, Bratislava, 298 p. (in Slovak with English summary).
- Bakos, F., Fuchs, P., Hanes, R., Žitňan, P. & Konečný, V. 2010. Au-porphyry mineralization in the mantle of the Štiavica stratovolcano (Western Carpathians). *Mineralia Slovaca*, **42**, 1-14.
- Bartalský, B. & Finka, O. 1999. New results of the geological exploration of the 1st vein system of the Kremnica precious metal veins. *Mineralia Slovaca*, **31**, 291-296 (in Slovak).
- Blundy, J., Cashman, K. & Humphreys, M. 2006. Magma heating by decompression-driven crystallization beneath andesite volcanoes. *Nature*, **443**, 76-80.
- Bodnar, R. J. 1993. Revised equation and table for determining the freezing point depression of H₂O-NaCl solutions. *Geochimica et Cosmochimica Acta*, **57**, 683-684.
- Böhmer, M. 1966. Geology and mineral associations of gold-bearing veins in the central part of the Kremnica ore field. *Acta Geologica et Geographica Universitatis Comeniana, Geologica*, **11**, 5-123 (in Slovak).
- Böhmer, M., Gerthofferová H. & Kraus, I. 1969. To the problems of alterations of central Slovakia Neovolcanites. *Geologický Zborník Geologica Carpathica*, **20**, 47-68.
- Böhmer, M. 1977. Deep structures of the Kremnica ore field. Open file report, Archive of the State Geological Institute of D. Štúr, Bratislava (in Slovak).
- Böhmer, M. & Škvarka L. 1970. The relationship between footwall of Neogene volcanic rocks and effluences of thermal water in Kremnica. *Geologické práce, správy*. **53**, 21-32 (in Slovak).
- Bottinga, Y. & Javoy M. 1973. Comments on oxygen isotope geothermometry. *Earth and Planetary Science Letters*, **20**, 250-265.
- Boullier, A. M. & Robert, F. 1992. Paleoseismic events recorded in Archean gold-quartz vein networks, Val d'Or, Abitibi, Quebec, Canada. *Journal of Structural Geology*, **14**, 161-179.

- Capuano, R. M. 1992. The temperature-dependence of hydrogen isotope fractionation between clay minerals and water: Evidence from a geopressured system. *Geochimica et Cosmochimica Acta*, **56**, 2547-2554.
- Chacko, T., Mayeda, T. K., Clayton, R. N. & Goldsmith, J. R. 1991. Oxygen and carbon isotope fractionations between CO₂ and calcite. *Geochimica et Cosmochimica Acta*, **55**, 2867-2882
- Chernyshev, I. V., Konečný, V., Lexa, J., Kovalenker, V. A., Jeleň, S., Lebedev, V. A. & Goltsman, Yu. V. 2013: K-Ar and Rb-Sr geochronology and evolution of the Štiavnica Stratovolcano, Central Slovakia. *Geologica Carpathica*, **64**, 327-351.
- Clayton, R. N. & Keiffer, S. W. 1991. Oxygen isotopic thermometer calibrations. In: Taylor, H. P., O'Neil, J. R. & Kaplan, I. R. (eds) *Stable Isotope Geochemistry: A Tribute to Samuel Epstein*. The Geochemical Society, Special Publications, **3**, 3-10.
- Cooke, D. R. & Simmons, S. F. 2000. Characteristics and genesis of epithermal gold deposits. In: Hagemann G., Brown P. E. (eds) *Gold in 2000*. Reviews in Economic Geology, **13**, 221-244.
- Doppler, G., Bakker, R. J. & Baumgartner, M. 2013. Fluid inclusion modification by H₂O and D₂O diffusion: the influence of inclusion depth, size, and shape in re-equilibration experiments. *Contributions to Mineralogy and Petrology*, **165**, 1259-1274.
- Dudek, T. & Środoń, J. 1996. Identification of illite/smectite by X-ray powder diffraction taking into account the lognormal distribution of crystal thickness. *Geologica Carpathica-Clays*, **5**, 21-32.
- Essene, E. J. & Peacor, D. R. 1995. Clay mineral thermometry; a critical perspective. *Clays and Clay Minerals*, **43**, 540-553.
- Fallick, A. E., Macaulay, C. I. & Haszeldine, R. S. 1993. Implications of linearly correlated oxygen and hydrogen isotopic compositions for kaolinite and illite in the Magnus Sandstones, North Sea. *Clays and Clay Minerals*, **41**, 184-190.
- Faure, K. 2003. δD values of fluid inclusion water in quartz and calcite ejecta from active geothermal systems: Do values reflect those of original hydrothermal water? *Economic Geology*, **98**, 657-660.
- Field, C. W. & Fifarek, R. H. 1985. Light stable isotope systematics in the epithermal environment. In: Berger, B. R. & Bethke, P. M. (eds) *Geology and geochemistry of epithermal systems*. Reviews in Economic Geology, Society of Economic Geologists, Littleton, **2**, 99-128.
- Finka, O. 2009. Wealth hidden in earth, history and present of the gold deposit in Kremnica. Krupa print, s.r.o., Žilina, 196 p. (in Slovak with English summary).
- Fournier, R. O. 1985. The behavior of silica in hydrothermal solutions. In: Berger, B. R. & Bethke, P. M. (eds) *Geology and geochemistry of epithermal systems*. Reviews in Economic Geology, Society of Economic Geologists, Littleton, **2**, 45-61.
- Fournier, R. O. 1999. Hydrothermal processes related to movement of fluid from plastic into brittle rock in the magmatic-epithermal environment. *Economic Geology*, **94**, 1193-1212.
- Friedman, I. & O'Neil, J. R. 1977. Compilation of stable isotope fractionation factors of geochemical interest. In: Fleischer, M. (ed) *Data of Geochemistry*, U. S. Geological Survey Professional Papers, 440-KK, 49 p.
- Giggenbach W. F. 1992. Isotopic shifts in waters from geothermal and volcanic systems along convergent plate boundaries and their origin. *Earth and Planetary Science Letters*, **113**, 495-510.
- Gilg, H. A. & Sheppard, S. M. F. 1996. Hydrogen isotope fractionation between kaolinite and water revisited. *Geochimica et Cosmochimica Acta*, **60**, 529-533.
- Goldstein, R.H. & Reynolds, T.J. 1994. Systematics of fluid inclusions in diagenetic minerals. Society of Sedimentary Geology Short Course, **31**, 199 p.
- Golyshev, S. I., Padalko, N. L. & Pechenkin, S. A. 1981. Fractionation of stable oxygen and carbon isotopes in carbonate systems. *Geochemistry International*, **18**, 85-99.
- Haas, J. L. 1971. The effect of salinity on the maximum thermal gradient of a hydrothermal system at hydrostatic pressure. *Economic Geology*, **66**, 940-946.
- Haas, J. L. 1976. Physical properties of the coexisting phases and thermochemical properties of the H₂O component in boiling NaCl solutions. U.S. Geological Survey Bulletin 1421-B, 71 p.
- Háber, M., Jeleň, S., Kovalenker, V. & Černyšev, I. 2001. Model of epithermal ore mineralization of the Banská Štiavnica ore district. *Mineralia Slovaca*, **33**, 215-224 (in Slovak).

- Hanes, R., Bakos, F., Fuchs, P., Žitňan, P. & Konečný, V. 2010. Exploration results of Au porphyry mineralizations in the Javorie Stratovolcano. *Mineralia Slovaca*, **42**,15-33.
- Harangi, Sz. & Lenkey, L. 2007. Genesis of the Neogene to Quaternary volcanism in the Carpathian–Pannonian region: Role of subduction, extension, and mantle plume. *Geological Society of America Special Papers*, **418**, 67-92.
- Harvey, C. C. & Browne P. R. L. 2000. Mixed-layer clays in geothermal systems and their effectiveness as mineral geothermometers. Proceedings of the World Geothermal congress, Kyushu, Japan, 1201-1205.
- Hedenquist, J. W. & Arribas, A. Jr. 1999. Epithermal gold deposits: I. Hydrothermal activity and processes, and II. Characteristics and genesis of epithermal deposits. In: Molnár, F., Lexa, J. & Hedenquist, J. W. (eds) *Epithermal mineralization of the Western Carpathians*. Guidebook series of the Society of Economic Geologists, **31**, 13-64.
- Hedenquist, J. W. & Henley, R. W. 1985. Effect of CO₂ on freezing point depression measurements on fluid inclusions: evidence from active geothermal systems and applications to epithermal studies. *Economic Geology*, **80**, 1379-1406.
- Hedenquist, J. W. & Lowenstern J. B. 1994. The role of magmas in the formation of hydrothermal ore deposits. *Nature*, **370**, 519-527.
- Hedenquist, J. W., Izawa, E., Arribas, A. & White, N. C. 1996. Epithermal gold deposits: Styles, characteristics, and exploration. The Society of Resource Geology Special Publications, **1**, 16 p.
- Hedenquist, J. W., Arribas, A. & Gonzalez-Urien, E. 2000. Exploration for epithermal gold deposits In: Hagemann, S. G. & Brown, P. E. (eds) *Gold in 2000*. Reviews in Economic Geology, Society of Economic Geologists, Littleton, **13**, 245-277.
- Heinrich, C. A. 2005. The physical and chemical evolution of low-salinity magmatic fluids at the porphyry to epithermal transition: a thermodynamic study. *Mineralium Deposita*, **39**, 864-889.
- Holtz, F., Johannes, W., Tamic, N. & Behrens, H. 2001. Maximum and minimum water contents of granitic melts: a reexamination and implications. *Lithos*, **56**, 1-14.
- Holtz, F., Sato, H., Lewis, J., Behrens, H. & Nakada, S. 2005. Experimental Petrology of the 1991–1995 Unzen Dacite, Japan. Part I: Phase Relations, Phase Composition and Pre-eruptive Conditions. *Journal of Petrology*, **46**, 319-337.
- Horita, J. & Wesolowski, D. J. 1994. Liquid-vapor fractionation of oxygen and hydrogen isotopes of water from the freezing to the critical temperature. *Geochimica et Cosmochimica Acta*, **58**, 3425-3437.
- Hu, G. X. & Clayton, R. N. 2003. Oxygen isotope salt effects at high pressure and high temperature and the calibration of oxygen isotope geothermometers. *Geochimica et Cosmochimica Acta*, **67**, 3227-3246.
- IAEA 1992. Statistical treatment of data on environmental isotopes in precipitation. International Atomic Energy Agency, Vienna, Technical Reports Series, **331**, 781 p.
- Jackson, M.I. 1975. Soil Chemical Analysis – Advanced Course. Madison, Wisconsin.
- Koděra, P. & Lexa, J. 2003. Metalogeny of the Au deposit Banská Hodruša I. Open file report, Archive of the State Geological Institute of D. Štúr, Bratislava (in Slovak).
- Koděra, P. & Lexa, J. 2010. Classic localities in Central Slovakia Volcanic Field: Gold, silver and base metal mineralizations and mining history at Banská Štiavnica and Kremnica. *Acta Mineralogica-Petrographica, Field Guide Series*, **29**, 19 p.
- Koděra, P., Lexa, J., Rankin, A. H. & Fallick, A. E. 2004. Fluid evolution in a subvolcanic granodiorite pluton related to Fe and Pb-Zn mineralization, Banská Štiavnica ore district, Slovakia. *Economic Geology*, **99**, 1745-1770.
- Koděra, P., Lexa, J., Rankin, A. H. & Fallick, A. E. 2005. Epithermal gold veins in a caldera setting: Banská Hodruša, Slovakia. *Mineralium Deposita*, **39**, 921-943.
- Koděra, P., Šucha, V., Lexa, J. & Fallick, A. E. 2007. The Kremnica Au-Ag epithermal deposit: an example of laterally outflowing hydrothermal system? In: Andrew, C. J. et al. (eds) *Digging Deeper*. Proceedings of the 9th SGA Biennial Meeting, Irish Association for Economic Geology, 173-176.
- Koděra, P., Lexa, J., Biroň, A. & Žitňan, J. 2010a. Gold mineralization and associated alteration

zones of the Biely vrch Au-porphyry deposit, Slovakia. *Mineralia Slovaca*, **42**, 33-56.

Koděra, P., Lexa, J. & Fallick, A. E. 2010b. Formation of the Vysoká-Zlatno Cu-Au skarn-porphyry deposit, Slovakia. *Mineralium Deposita*, **45**, 817-843.

Koděra, P., Lexa, J., Heinrich, C. A., Wälle, M. & Fallick, A. E. 2011. Au mineralisation at Biely Vrch deposit (W Carpathians, Slovakia): example of a very shallow porphyry system. In: Barra, F., Reich, M., Campos, E. & Tornos, F. (eds) *Let's Talk Ore Deposits*. Proceedings of 11th SGA Biennial Meeting, Ediciones Universidad Católica del Norte, Antofagasta, Chile, 417-419.

Koděra, P., Lexa, J. & Konečný, P. 2013: Application of CL-imaging and mineral geothermometry on the porphyry gold deposit Biely Vrch, Slovakia: in Proceedings of 12th SGA Biennial Meeting, Uppsala, Sweden (in press).

Konečný, P. 2002. Evolution of magmatic reservoir underneath the Štiavnica stratovolcano. PhD thesis, Comenius University, Bratislava, 273 p. (in Slovak).

Konečný, V., Lexa, J. & Hojstřičová, V. 1995. The Central Slovakia Neogene volcanic field: a review. *Acta Vulcanologica*, **7**, 63-78.

Konečný, V., Bezák, V., Halouzka, R., Konečný, P., Mihaliková, A., Marcin, D., Iglárová, L., Panáček, A., Štohl, J., Žáková, E., Galko, I., Rojkovičová, L. & Onačila, D. 1998a. Explanation to the geological map of Javorie 1 : 50 000. Geological Survey of Slovak Republic, Bratislava, 304 p. (in Slovak with English summary).

Konečný, V., Lexa, J., Halouzka, R., Hók, J., Vozár, J., Dublan, L., Nagy, A., Šimon, L., Havrila, M., Ivanička, J., Hojstřičová, V., Mihaliková, A., Vozárová, A., Konečný, P., Kováčiková, M., Filo, M., Marcin, D., Klukanová, A., Liščák, P. & Žáková, E. 1998b. Explanatory notes to the geological map of Štiavnické and Pohronský Inovec mountain ranges (Štiavnica stratovolcano). Geological Survey of Slovak Republic, Bratislava, 472 p. (in Slovak with English summary).

Konečný, V., Kováč, M., Lexa, J. & Šefara, J. 2002. Neogene evolution of the Carpatho-Pannonian region: an interplay of subduction and back-arc diapiric uprising in the mantle. *EGU Stephan Mueller Special Publication Series*, **1**, 165-194.

Kovačič, V. 2010. Comparison of vein systems Krížne veins and Kirchberg vein in northern part of the Kremnica hydrothermal system. MSc thesis, Comenius University, Bratislava, 88 p.

Kraus, I., Šamajová, E., Šucha, V., Lexa, J. & Hroncová, Z. 1994. Diagenetic and hydrothermal alterations of volcanic rocks into clay minerals and zeolites (Kremnické Vrchy Mts., the Western Carpathians). *Geologica Carpathica*, **45**, 151-158.

Kraus, I., Chernishev, I. V., Šucha, V., Kovalenker, V. A., Lebedev, V. A. & Šamajová, E. 1999. Use of illite for K/Ar dating of hydrothermal precious and base metal mineralization in central Slovak Neogene volcanic rocks. *Geologica Carpathica*, **50**, 353-364.

Kubač, A. 2013. Mineralogy of precious metal – base metal vein mineralisation at the Rozália mine (Štiavnica stratovolcano). MSc thesis, Comenius University, Bratislava, 68 p.

Lexa, J., 2000. Metallogeny of the Central Slovakia Volcanic Field. *Mineralia Slovaca*, **32**, 251-256.

Lexa, J. & Konečný, V. 1998. Geodynamic aspects of the Neogene to Quaternary volcanism. In: Rakús, M. (ed) *Geodynamic development of the Western Carpathians*. Geological Survey of Slovak Republic, Bratislava, 219-240.

Lexa, J., Konečný, P., Hojstřičová, V., Konečný, V. & Köhlerová, M. 1998a. Petrologic model of the Štiavnica stratovolcano, Central Slovakia Neogene Volcanic Field. Abstracts of the XVIth congress CBGA, Vienna, 340.

Lexa, J., Halouzka, R., Havrila, M., Hanzel, V., Kubeš, P., Liščák, P. & Hojstřičová, V. 1998b. Explanatory notes to the geological map of the Kremnické vrchy mountain range. Geological Survey of Slovak Republic, Bratislava, 308 p. (in Slovak with English summary).

Lexa, J., Štohl, J., Konečný, V. & V. 1999a. Banská Štiavnica ore district: relationship among metallogenetic processes and the geological evolution of a stratovolcano. *Mineralium Deposita*, **34**, 639-665.

Lexa, J., Koděra P., Prcúch, J., Veselý, M. & Šály, J. 1999b. Multiple stages of mineralization at the Rozália Mine, Hodruša. In: Molnár, F., Lexa, J. & Hedenquist, J. W. (eds) *Epithermal mineralization of the Western Carpathians*. Guidebook series of the Society of Economic Geologists, **31**, 229-247.

Lexa, J., Konečný, P. & Koděra, P. 2012. Some petrological aspects of parental intrusion of the Au-porphyry deposit Biely vrch near Detva. Proceedings of the conference Geochémia 2012, State Geological Institute of D. Štúr, Bratislava, 100-103 (in Slovak).

Macaulay, C. I., Fallick, A. E., Haszeldine, R.S. & Graham C. M. 2000. Methods of laser-based stable isotope measurement applied to diagenetic cements and hydrocarbon reservoir quality. *Clay Minerals*, **35**, 313-322.

Maťo, L., Sasvári, T., Bebej, J., Kraus, I., Schmidt, R. & Kalinaj, M. 1996. Structurally-controlled vein-hosted mesothermal gold-quartz and epithermal precious/base-metal mineralization in the Hodruša ore field, Central Slovakia Volcanic Field. *Mineralia Slovaca*, **28**, 455-490 (in Slovak with English abstract).

Maťo, L. 1997. Partial report at the project Kremnica – Horná Ves, VP, Au – Ag ores. Mineralogical report - Appendix E2. Open file report, Archive of the State Geological Institute of D. Štúr, Bratislava (in Slovak).

Matsuhisa, Y., Goldsmith, J. R. & Clayton, R. N. 1979. Oxygen isotopic fractionation in the system quartz-albite-anorthite-water. *Geochimica et Cosmochimica Acta*, **43**, 1131-1140.

Müller, A., Herrington, R., Armstrong, R., Seltman, R., Kirwin, D., Stenina, N. & Kronz, A. 2010. Trace elements and cathodoluminescence of quartz in stockwork veins of Mongolian porphyry-style deposits. *Mineralium Deposita*, **45**, 707-727.

Muntean, J. L. & Einaudi, M. T. 2000. Porphyry gold deposits of the Refugio district, Maricunga belt, northern Chile. *Economic Geology*, **95**, 1445-1472.

Muntean, J. L. & Einaudi, M. T. 2001. Porphyry-epithermal transition: Maricunga belt, northern Chile. *Economic Geology*, **96**, 743-772.

Nemčok, M., Hók, J., Kováč, P., Marko, F., Madarás, J. & Bezák, V. 1993. Tectonics of Western Carpathians during Tertiary (in Slovak). In: Rakús, M. & Vozár, J. (eds) *Geodynamic model and deep structure of the Western Carpathians*. D. Štúr Institute of Geology, Bratislava, 263 – 268 (in Slovak).

Ohmoto, H., Goldhaber, M. B. 1997. Sulfur and carbon isotopes. In: Barnes, H. L. (ed) *Geochemistry of hydrothermal ore deposits*. 3rd ed., Wiley Interscience, New York, 517-611.

Ohmoto, H., Rye, R. O. 1979. Isotope of sulfur and carbon. In: Barnes, H. L. (ed), *Geochemistry of hydrothermal deposits*. John Wiley & Sons, 509-567.

Onačiča, D., Lexa, J., Marsina, K., Rojkovičová, L., Káčer, Š., Hojstričová, V., Žáková, E., Štohl, J., Konečný, V., Nemčok, M., Koděra, P., Konečný, P., Repčok, I., Hurai, V., Háber, M., Jeleň, S., Maťo, L., Sasvári, T., Schmidt, R., Zvara, I. & Grant, T. 1995. Metallogenetic model and resource assessment of the Štiavnica stratovolcano central zone. Open file report, Archive of the State Geological Institute of D. Štúr, Bratislava, 231 p. (in Slovak).

Pécskay, Z., Lexa, J. & Molnár, F., 2010. Relationships of rhyolite magmatism and epithermal systems in the Central Slovakia and Tokaj Mts. regions of the Western Carpathians: K/Ar dating of volcanic and hydrothermal processes. In: *Acta Mineralogica-Petrographica*, Abstract Series, **6**, 297.

Planderová, E., Ziemińska-Tworzydło, M., Grabowska, I., Kohlman-Adamska, A., Konzálová, M., Nagy, E., Pantić, N., Ryłova, T., Sadowska, A., Słodkowska, B., Stuchlik, L., Syabryaj, S., Wazynska, H. & Zdražilková, N. 1993. On paleofloristic and paleoclimatic changes during the Neogene of Eastern and Central Europe on the basis of palynological research. In: *Paleofloristic and paleoclimatic changes during Cretaceous and Tertiary*. Proceedings of International Symposium, D. Štúr Institute of Geology, Bratislava, 119-129.

Reyes, A. G., 1990. Petrology of Philippine geothermal systems and the application on the alteration mineralogy to their assessment. *Journal of Volcanology and Geothermal Research*, **43**, 279-309.

Roedder, E. 1984. Fluid inclusions. *Reviews in Mineralogy*, Mineralogical Society of America, **12**, 644 p.

Royden, L. H., Horváth, F. & Burchfield, B. C. 1982. Transform faulting, extension, and subduction in the Carpathian Pannonian region. *Geological Society of America Bulletin*, **93**, 717-725.

Salter, J. M., Hart, S. R. & Pantó, G. 1988. Origin of late Cenozoic volcanic rocks of the Carpathian arc, Hungary. In: Royden, L. & Horváth, F. (eds): *The Pannonian Basin. A study in basin*

evolution. American Association of Petroleum Geologists, Memoir, **45**, 279-292.

Šály, J., & Prcúch, J. 1999. Structural-tectonic and mineralogical conditions of Au mineralization at the Rozália mine (Hodruša-Hámre). *Mineralia Slovaca*, **3-4**. 315-316 (in Slovak).

Šály, J., Hók, J., Lepeň, I., Okál', M., Reck, V. & Varga, P. 2008. Exploration of bodies with precious metal mineralisation in the vicinity of the deposit Hodruša – Svetozár. Final report with calculation of reserves. Confidential report, Archive of the State Geological Institute of D. Štúr, Bratislava (in Slovak).

Savin, S. M. & Lee, M. 1988. Isotopic studies of phyllosilicates. In: Bailey, S.W. (ed) *Hydrous Phyllosilicates*. Mineralogical Society of America, Reviews in Mineralogy, **19**, 189-223.

Seedorf, E., Dilles, J. H., Phoffett Jr, J. M., Einaudi, M. T., Zurcher, L., Stavast, W. J. A., Johnson, D. A. & Barton, M. D. 2005: Porphyry deposits: Characteristics and origin of hypogene features. In: Hedenquist, J. W., Thompson, J. F. H., Goldfarb, R. J. & Richards, J. P. (eds.), *Economic Geology 100th Anniversary Volume 1905-2005*. Society of Economic Geologists, Littleton, 251-298.

Seghedi, I. & Downes, H. 2011. Geochemistry and tectonic development of Cenozoic magmatism in the Carpathian–Pannonian region. *Gondwana Research*, **20**, 655-672.

Seward, T. M. 1989. The hydrothermal chemistry of gold and its implications for ore formation: boiling and conductive boiling as examples. In: Keays, R. R., Ramsay, R. W. H. & Groves, D. I. (eds) *The geology of gold deposits: The perspective in 1988*. Society of Economic Geologists, Economic Geology Monographs, **6**, 398-404.

Sharp, Z. D. & Kirschner, D. L. 1994. Quartz-calcite isotope geothermometry: A calibration based on natural isotopic variations. *Geochimica et Cosmochimica Acta*, **58**, 4491-4501.

Shepherd, T. J., Rankin, A. H. & Alderton, D. H. M. 1985. *A practical guide to fluid inclusion studies*. Blackie & Son, London, 235 p.

Sheppard, S. M. F. 1986. Characterization and isotopic variations in natural waters. In: Valley, J. W., Taylor, H. P. Jr., O'Neil, J. R. (ed) *Stable isotopes in high temperature geological processes*. Mineralogical Society of America, Reviews in Mineralogy, **16**, 165-184.

Sheppard, S. M. F. & Gilg, H. A. 1996. Stable isotope geochemistry of clay minerals. *Clay Minerals*, **31**, 1-24.

Sibson, R. H., Robert, F. & Poulsen, H. 1988. High angle faults, fluid pressure cycling and mesothermal gold-quartz deposits. *Geology*, **16**, 551-555.

Sillitoe, R. H. 1993. Epithermal models: Genetic types, geometrical controls and shallow features. In: Kirkham, R. V., Sinclair, W. D., Thorpe, R. I., Duke, J. M. (eds) *Mineral deposit modeling*. Geological Association of Canada, Special Papers, **40**, 403-417.

Sillitoe, R. H. 2010. Porphyry copper systems. *Economic Geology*, **105**, 3-41.

Sillitoe, R. H. & Hedenquist, J. W. 2003. Linkages between volcanotectonic settings, ore-fluid compositions, and epithermal precious metal deposits. In: Simmons, S. F., Graham, I. (eds) *Volcanic, geothermal, and ore-forming fluids: Rulers and witnesses of processes within the earth*. Society of Economic Geologists, Economic Geology Special Publications, **10**, 315-343.

Simmons, S. F. 1995. Magmatic contributions to low-sulfidation epithermal deposits. In: Thompson, J. F. H. (ed) *Magmas, fluids and ore deposits*. Mineralogical Association of Canada, Short Course Series, **23**, 455-477.

Simmons, S. F. & Browne, P. R. L. 1997. Saline fluid inclusions in sphalerite from the Broadlands-Ohaaki geothermal system: A coincidental trapping of fluids being boiled toward dryness. *Economic Geology*, **92**, 485-489.

Simmons, S. F., White, N. C. & John, D. 2005. In: Hedenquist, J. W., Thompson, J. F. H., Goldfarb, R. J. & Richards, J. P. (eds.), *Economic Geology 100th Anniversary Volume 1905-2005*. Society of Economic Geologists, Littleton, 485-522.

Simon, K. 2001. Does δD from fluid inclusion in quartz reflect the original hydrothermal fluid? *Chemical Geology*, **177**, 483-495.

Simpson, M. P., Mauk, J. L., Simmons & S. F. 2001. Hydrothermal alteration and hydrologic evolution of the Golden Cross epithermal Au-Ag deposit, New Zealand. *Economic Geology*, **96**, 773-796.

Slovak minerals yearbook. 2003. Baláž, P. & Tréger, M. (eds), State Geological Institute of D.

- Štúr, Bratislava, 1-175 (in Slovak)
- Slovak minerals yearbook. 2008. Baláž, P. & Kúšik, D. (eds), State Geological Institute of D. Štúr, Bratislava, 1-163 (in Slovak).
- Slovak minerals yearbook. 2011. Baláž, P. & Kúšik, D. (eds), State Geological Institute of D. Štúr, Bratislava, 1-155 (in Slovak).
- Środoń, J. 1980. Precise identification of illite/smectite interstratifications by X-ray powder diffraction. *Clays and Clay Minerals*, **28**, 401–411.
- Środoń, J. 1984. X-ray powder diffraction identification of illitic materials. *Clays and Clay Minerals*, **32**, 337–349.
- Steele-MacInnis, M., Bodnar, R. J. & Naden, J., 2011: Numerical model to determine the composition of H₂O-NaCl-CaCl₂ fluid inclusions based on microthermometric and microanalytical data. *Geochimica et Cosmochimica Acta*, **75**, 21-40.
- Sterner, S. M., Hall, D. L., Bodnar, R. J. 1988. Synthetic fluid inclusions. V. Solubility relations in the system NaCl-KCl-H₂O under vapor-saturated conditions. *Geochimica et Cosmochimica Acta*, **52**, 989-1006.
- Stoffregen, R. E., Rye, R. O. & Wasserman, M. D. 1994. Experimental studies of alunite: Part I, ¹⁸O-¹⁶O and D-H fractionation factors between alunite and water at 250-450°C. *Geochimica et Cosmochimica Acta*, **58**, 903-916.
- Šály, J., Hók, J., Lepeň, I., Okál', M., Reck, V. & Varga, P., 2008: Exploration of Au mineralization in surroundings of the Hodruša – Svätozár deposit; final report with reserve estimate. Open file report, Archive of the State Geological Institute of D. Štúr, Bratislava (in Slovak).
- Štohl, J., Lexa, J., Kaličiak, M. & Bacsó, Z. 1994. Metallogeny of stockwork base metal mineralizations in Neogene volcanics of Western Carpathians. *Mineralia Slovaca*, **26**, 75-117 (in Slovak with English summary).
- Šucha, V., Kraus, I., Gerthofferová, H., Peteš, J. & Sereková, M. 1992. Smectite to illite conversion in bentonites and shales of the East Slovak basin. *Clay Minerals*, **28**, 243-253.
- Suzuoki, T. & Epstein, S. 1976. Hydrogen isotope fractionation between OH-bearing minerals and water. *Geochimica et Cosmochimica Acta*, **40**, 1229-1240.
- Taylor, B. E. 1992. Degassing of H₂O from rhyolite magma during eruption and shallow intrusion, and the isotopic composition of magmatic water in hydrothermal systems. In: Hedenquist, J. W. (ed) *Magmatic contributions to hydrothermal systems*. Geological Survey of Japan, Reports, **279**, 190-194.
- Taylor, H. P. Jr. 1997. Oxygen and hydrogen isotope relationships in hydrothermal mineral deposits. In: Barnes, H. L. (ed) *Geochemistry of hydrothermal ore deposits*. 3rd ed., Wiley Interscience, New York, 229-303.
- Thomas, J. B., Watson, E. B., Spear, F. S., Shemella, P. T., Nayak, S. K. & Lanzirotti, A. 2010. Titanite under pressure: the effect of pressure and temperature on the solubility of Ti in quartz. *Contribution to Mineralogy and Petrology*, **160**, 743-759.
- Uhlík, P. & Majzlan J. 2004. Conditions of mixed-layer illite-smectite formation at the deposit Dolná Ves on the southwest margin of Kremnica stratovolcano. *Mineralia Slovaca*, **36**, 331-338.
- Veľký, P. 1992. Final report with calculation of reserves on project: Kremnické Bane - Šturec-north, Au, Ag ores. Open file report, D. Štúr Institute of Geology, Bratislava (in Slovak).
- Veľký, P., Böhmer, M., Korim, M., Maťo, L., Pitoňák, P., Oroszlány, J., Padúch, M., Dimoš, I. & Versegny, R. 1998. Complex evaluation of the precious metal ore deposit Kremnica. Final report. Open file report, Archive of the State Geological Institute of D. Štúr, Bratislava (in Slovak).
- Wilkinson, J. J. 2001. Fluid inclusions in hydrothermal ore deposits. *Lithos*, **55**, 229-272.
- Williams-Jones, A. E. & Heinrich, C. A. 2005. Vapor transport of metals and the formation of magmatic-hydrothermal ore deposits. *Economic Geology*, **100**, 1287-1312.
- Zajacz, Z., Candela P. A., Piccoli, P. M. & Sanchez-Valle, C. 2012. The partitioning of sulfur and chlorine between andesite melts and magmatic volatiles and the exchange coefficients of major cations. *Geochimica et Cosmochimica Acta*, **89**, 81–101.
- Zaluski, G., Nesbitt, B. E. & Muehlenbachs, K. 1994. Hydrothermal alteration and stable isotope systematics of the Babine porphyry Cu deposits, British Columbia: Implications for fluid evolution of porphyry systems. *Economic Geology*, **89**, 1518-1541.

Zheng, Y. F. & Simon, K. 1991. Oxygen isotope fractionation in hematite and magnetite: A theoretical calculation and application to geothermometry of metamorphic iron-formation. *European Journal of Mineralogy*, **3**, 877-886.

Zheng, Y. F. 1993. Calculation of oxygen isotope fractionation in anhydrous silicate minerals. *Geochimica et Cosmochimica Acta*, **57**, 1079-1091.

Žitňan, J. 2010. Characteristic of alteration of advanced argillic type at the localities Biely Vrch and Kalinka in Javorie. MSc thesis, Comenius University, Bratislava, 108 p.